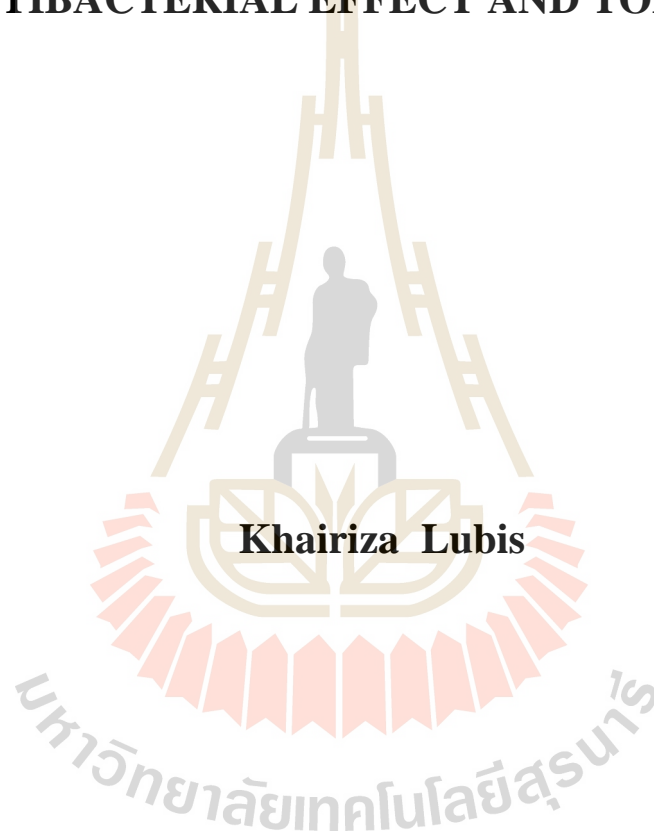


**CHARACTERIZATION OF GOLD NANOPARTICLES
SYNTHESIZED BY USING *CURCUMA XANTHORRHIZA*
AND EVALUATION OF THEIR CATALYTIC ACTIVITY,
ANTIBACTERIAL EFFECT AND TOXICITY**



**A Thesis Submitted in Partial Fulfillment of the Requirements for the
Degree of Doctor of Philosophy in Environmental Biology
Suranaree University of Technology**

Academic year 2017

การตรวจสอบคุณลักษณะของอนุภาคทองคำที่สังเคราะห์ด้วย
CURCUMA XANTHORRHIZA และการประเมินฤทธิ์
เร่งปฏิกิริยา ฤทธิ์ต้านแบคทีเรียและการเกิดพิษ

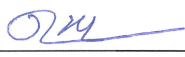


วิทยานิพนธ์นี้เป็นส่วนหนึ่งของการศึกษาตามหลักสูตรปริญญาวิทยาศาสตรดุษฎีบัณฑิต
สาขาวิชาชีววิทยาสิ่งแวดล้อม
มหาวิทยาลัยเทคโนโลยีสุรนารี
ปีการศึกษา 2560

**CHARACTERIZATION OF GOLD NANOPARTICLES
SYNTHESIZED BY USING *CURCUMA XANTHORRHIZA* AND
EVALUATION OF THEIR CATALYTIC ACTIVITY,
ANTIBACTERIAL EFFECT AND TOXICITY**


Suranaree University of Technology has approved this thesis submitted in fulfillment of the requirements for the Degree of Doctor of Philosophy.

Thesis Examining Committee



(Asst. Prof. Dr. Duangkamol Maensiri)

Chairperson



(Assoc. Prof. Dr. Nuannoi Chudapongse)

Member (Thesis Advisor)



(Dr. Pongrit Krubprachaya)

Member



(Asst. Prof. Apiwat Chompoosor)

Member



(Dr. Oratai Weeranantanapan)

Member



(Asst. Prof. Dr. Worawat Meevasana)



(Prof. Dr. Santi Maensiri)

Vice Rector for Academic Affair
and Internationalization

Dean of Institute of Science

ไครีชา ลูบิส : การตรวจสอบคุณลักษณะของอนุภาคทองคำนาโนที่สังเคราะห์ด้วย *CURCUMA XANTHORRHIZA* และการประเมินฤทธิ์เร่งปฏิกิริยา ฤทธิ์ต้านแบคทีเรียและการเกิดพิษ (CHARACTERIZATION OF GOLD NANOPARTICLES SYNTHESIZED BY USING *CURCUMA XANTHORRHIZA* AND EVALUATION OF THEIR CATALYTIC ACTIVITY, ANTIBACTERIAL EFFECT AND TOXICITY).

อาจารย์ที่ปรึกษา : รองศาสตราจารย์ ดร.นวลน้อย จุฑะพงษ์, 71 หน้า.

ในการศึกษานี้ การสังเคราะห์อนุภาคนาโนแบบประหยัด เป็นมิตรต่อระบบนิเวศและสิ่งแวดล้อมถูกนำมาใช้ในการผลิตอนุภาคทองคำนาโนด้วยสารสกัดจาก *Curcuma xanthorrhiza* ซึ่งเป็นพืชเครื่องเทศที่ปลูกในประเทศอินโดนีเซีย สารสกัดน้ำจากเหง้าขมิ้นที่มีสถานะเป็นด่างซึ่งทำหน้าที่เป็นทั้งตัวรีดิวซ์และตัวคงสภาพถูกนำมาใช้ในการผลิตอนุภาคทองคำนาโนได้โดยสารสกัดจะไปทำให้เกิดปฏิกิริยารีดักชันของกรดเตตระคลอโรออร์ริก การเกิดอนุภาคทองคำนาโนสามารถสังเกตการเปลี่ยนสีของสารแขวนลอยด้วยตาเปล่าจากสีเหลืองอ่อนไปเป็นแดงทับทิม การเกิดอนุภาคทองคำนาโนที่เพิ่มขึ้นตามเวลาถูกติดตามเป็นระยะด้วยเทคนิค UV-visible spectroscopy พบว่า surface plasmon resonance ของอนุภาคทองคำนาโนสูงสุดที่ความยาวคลื่น 538 นาโนเมตร การกระจายของขนาดอนุภาคทองคำนาโนที่ผลิตขึ้น ณ อุณหภูมิห้องนาน 24 ชั่วโมง ถูกวัดด้วยวิธี dynamic light scattering (DLS) และพบว่า zeta potential มีประจุเป็นลบ ภาพถ่ายจากกล้องจุลทรรศน์อิเล็กตรอนแบบส่องกราดและแบบส่องผ่านทำให้ทราบว่าอนุภาคทองคำนาโนที่ได้จากการศึกษานี้ส่วนใหญ่มีรูปร่างกลมและคำนวณขนาดได้ 14.79 ± 3.65 นาโนเมตร ซึ่งสอดคล้องกับผลที่ได้จากวิธี X-ray diffraction (XRD) คือ 10 นาโนเมตร ธาตุที่เป็นส่วนประกอบในอนุภาคนาโนถูกวิเคราะห์ด้วย energy dispersive X-ray fluorescence (EDXRF) หมู่ฟังก์ชันในอนุภาคนาโนที่มาจากสารสกัดเหง้าขมิ้นเกี่ยวข้องกับกระบวนการเกิดปฏิกิริยาไบโอ-รีดักชันได้รับการยืนยันด้วยสเปกตรัมจากการวิเคราะห์ด้วยวิธี Fourier transform infrared (FTIR) spectroscopy

อนุภาคทองคำนาโนที่สังเคราะห์ได้ซึ่งมีความเข้มข้น 0.5 ไมโครกรัม/มิลลิลิตร มีฤทธิ์เร่งปฏิกิริยาการทำลายสีของโกเรดแต่ไม่พบฤทธิ์ต้านแบคทีเรียจากการทดสอบกับเชื้อแบคทีเรีย 4 สายพันธุ์ อนุภาคทองคำนาโนที่ผลิตขึ้นถูกนำไปทดสอบความเข้ากันได้กับเนื้อเยื่อสิ่งมีชีวิตภายนอก ร่างกายด้วยเซลล์สัตว์เลี้ยงลูกด้วยนม 3 ชนิด คือ เซลล์มะเร็งตับ HepG2 เซลล์มะเร็งเต้านม 4T1 และเซลล์ไฟโบรบลาสต์ของผิวหนัง HDFa จากการตรวจสอบการรอดชีวิตของเซลล์ด้วยวิธี Trypan blue exclusion พบว่าอนุภาคทองคำนาโนที่ผลิตได้ที่มีความเข้มข้นมากกว่าที่ใช้เป็นตัวเร่งปฏิกิริยาถึง 10 เท่าไม่ทำให้เกิดพิษต่อเซลล์ ผลการทดลองดังกล่าวคล้ายคลึงกับผลที่ได้จากการทดสอบในไข่

KHAIRIZA LUBIS : CHARACTERIZATION OF GOLD
NANOPARTICLES SYNTHESIZED BY USING *CURCUMA*
XANTHORRHIZA AND EVALUATION OF THEIR CATALYTIC
ACTIVITY, ANTIBACTERIAL EFFECT AND TOXICITY. THESIS
ADVISOR : ASSOC. PROF. NUANNOI CHUDAPONGSE, Ph.D. 71 PP.

GOLD/ NANOPARTICLE/ *CURCUMA XANTHORRHIZA*/ CATALYTIC/
ANTIBACTERIAL/ TOXICITY

In this study, an economical and environmentally friendly method, was chosen to produce gold nanoparticles (AuNPs) using *Curcuma xanthorrhiza*, a spice plant grown in Indonesia. Alkaline aqueous extract of *C. xanthorrhiza* rhizomes, which acts as reducing and stabilizing agent was used to produce AuNPs by bio-reduction of tetrachloroauric acid (HAuCl₄). The formation of AuNPs was visibly observed by the color change of the suspension from pale yellow to ruby-red. UV-visible spectroscopy was used to periodically monitor time-evolution. Surface plasmon resonance of the AuNPs suspension was found at a maximum absorption of 538 nm. At room temperature and 24-hour period of synthesis, size distribution was measured using dynamic light scattering (DLS). Zeta potential was found to be negative charge. Scanning electron microscope (SEM) and transmission electron microscope (TEM) images revealed that the Au-NPs obtained from this study mostly were spherical in shape and the calculated size was 14.79 ± 3.65 nm. In accordance with TEM data, the result from X-ray diffraction (XRD) showed that the average size of AuNPs was 10 nm. The elemental composition of nanoparticles was further determined by energy

dispersive X-ray fluorescence (EDXRF). The presence of functional groups derived from *C. xanthorrhiza* rhizomes extract involved in the gold bio-reduction process was confirmed by the spectrum of Fourier transform infrared (FTIR) spectroscopy.

The biosynthesized AuNPs at the concentration of 0.5 $\mu\text{g/ml}$ had catalytic activity in dye degradation of Congo red, however the antibacterial activity was not found in 4 strains of pathogens tested. *In vitro* biocompatibility of this biogenic AuNPs was evaluated in three types of mammalian cells, HepG2 (liver hepatocellular carcinoma), 4T1 breast cancer, and Human Dermal Fibroblast, adult (HDFa) cells. Cell viability of all cell lines by Trypan blue exclusion assay revealed that no toxicity was caused by the AuNPs at the concentration of 10 times higher than the catalytic concentration. Similarly, an *in vivo* toxicity study in zebrafish embryos showed no effect on mortality and hatching rate in the treated group compared to control when 1.25-5 $\mu\text{g/ml}$ of AuNPs were used. In conclusion, biocompatible AuNPs with catalytic activity was successfully fabricated with *C. xanthorrhiza* rhizomes extract by simple and non-expensive method. This catalytic activity of the obtained AuNPs will be useful for industrial applications as well as nanotechnology.

School of Biology

Academic Year 2017

Student's Signature Prof. 

Advisor's Signature 

ACKNOWLEDGEMENTS

The completion of this thesis could not have been possible without support and assistance from many people. I would like to express the deepest appreciation to my thesis advisor Assoc. Prof. Dr. Nuannoi Chudapongse for the continuous support of my Ph.D. study and related research, for her patience, motivation, and immense knowledge. Her guidance helped me in all the time of research and writing of this thesis. I could not have imagined having a better advisor and mentor for my Ph.D. study.

My sincere thanks also go to my thesis examining committee member, Asst. Prof. Dr. Duangkamol Maensiri, Dr. Pongrit Krubprachaya, Dr. Apiwat Chompoosor and Dr. Oratai Weeranantanapan for kindness and helpful suggestion for improving this thesis.

I am grateful to SUT-Ph.D. Scholarship Program for ASEAN for financial support.

In addition, I would like to thank God for providing me with the ability to complete the graduate program. My parents and my siblings for all their support and love, without them I would not be able to do anything.

Finally, my thanks also go to my friends for the stimulating discussion.

Khairiza Lubis

CONTENTS

	Page
ABSTRACT IN THAI.....	I
ABSTRACT IN ENGLISH	III
ACKNOWLEDGEMENTS.....	V
CONTENTS.....	VI
LIST OF TABLES	IX
LIST OF FIGURES	X
LIST OF ABBREVIATIONS.....	XII
CHAPTER	
I INTRODUCTION.....	1
1.1 Background/Problem.....	1
1.2 Research objectives	5
1.3 Research hypothesis.....	5
1.4 Scope and limitation of the study.....	5
II LITERATURE REVIEW	6
2.1 Study of AuNPs.....	6
2.2 Method for AuNPs synthesis	8
2.2.1 Turkevich method.....	9
2.2.2 Brust method	10
2.2.3 Seeded growth method	12

CONTENTS (Continued)

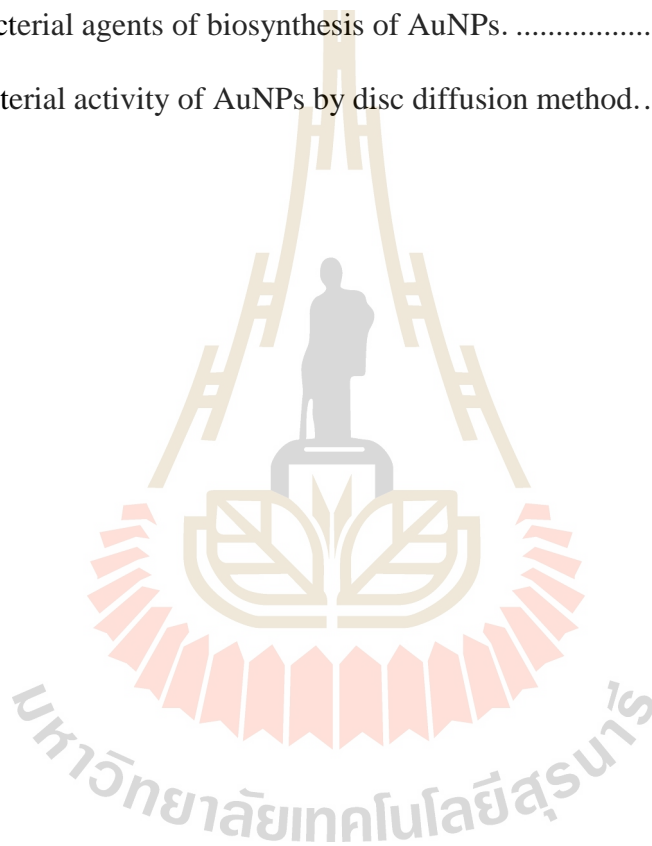
	Page
2.2.4 Biological synthesis by plant constituents.....	12
2.2.5 Synthesis method using microorganisms	13
2.2.6 Synthesis method using bio-molecules.....	14
2.3 Biosynthesis mechanism of metal nanoparticles.....	16
2.4 <i>Curcuma xanthorrhiza</i>	16
2.5 Cytotoxicity effect of AuNPs.....	18
2.6 Zebrafish model.....	20
2.7 Antibacterial activity of AuNPs	22
2.7.1 Antibacterial studies of AuNPs	22
2.7.2 The mechanism of nanoparticles toxicity against bacteria.....	22
III MATERIALS AND METHODS.....	24
3.1 Plant preparation and extraction.....	24
3.2 Synthesis and characterization of AuNPs	24
3.2.1 Synthesis.....	24
3.2.2 Characterization.....	25
3.3 Examination of catalytic activity of the synthesized AuNPs	26
3.4 Antibacterial test	27
3.5 Cytotoxicity assay	28
3.5.1 MTT assay.....	28
3.5.2 Trypan blue exclusion test.....	28

CONTENTS (Continued)

	Page
3.6 Zebrafish embryo toxicity test.....	29
3.6.1 Zebrafish rearing.....	29
3.6.2 Exposure protocol.....	29
3.7 Statistical analysis	29
IV RESULTS.....	30
4.1 UV-vis spectrophotometry analysis	30
4.2 X-ray diffraction.....	31
4.3 SEM, TEM and EDXRF studies	32
4.4 Particle size	33
4.5 FTIR analysis	35
4.6 Catalytic activity of the synthesized AuNPs.....	36
4.7 Antibacterial activity of AuNPs	38
4.8 Cytotoxicity study	40
4.9 <i>In vivo</i> study on zebrafish embryos.....	44
V DISCUSSION.....	45
REFERENCES	53
APPENDIX.....	68
CURRICULUM VITAE.....	71

LIST OF TABLES

Table	Page
2.1 Biosynthesis of AuNPs by using extract from part of plant.	15
2.2 Anti bacterial agents of biosynthesis of AuNPs.	22
4.1 Antibacterial activity of AuNPs by disc diffusion method.	38



LIST OF FIGURES

Figure	Page
2.1 The number of articles published on nanoparticles since 2001-2012.....	7
2.2 Technique for synthesis of nanoparticles.....	9
2.3 Illustration of the synthesis mechanism of AuNPs using citrate reduction method according to Turkevich method.	10
2.4 The synthetic steps involved in the Brust synthesis of AuNPs.....	11
2.5 Scheme of seeded growth method for synthesizing AuNPs	12
2.6 Biological synthesis by plant constituents	14
2.7 Mechanism of metal nanoparticle synthesis in plants extracts	16
2.8 <i>C. xanthorrhiza</i> rhizomes.....	18
2.9 Zebrafish life cycle.	21
2.10 The bactericidal illustration of AuNPs on <i>E. coli</i>	22
4.1 UV-visible absorption spectra of AuNPs synthesized by using <i>C. xanthorrhiza</i> rhizomes extract.....	31
4.2 X-ray diffraction pattern of AuNPs obtained from 1.5 ml of <i>C. xanthorrhiza</i> rhizomes extract at 24 h.....	32
4.3 SEM image of the AuNPs.....	33
4.4 TEM image and histogram.....	33
4.5 Energy dispersive spectra of AuNPs obtained from <i>C. xanthorrhiza</i> rhizomes extract.....	34

LIST OF FIGURES (Continued)

Figure	Page
4.6 The particle size distribution of AuNPs as measured by DLS.....	34
4.7 FTIR spectra of AuNPs synthesized by <i>C. xanthorrhiza</i> rhizomes extract and <i>C. xanthorrhiza</i> rhizomes powder.....	35
4.8 The absorbance of Congo red versus time.....	37
4.9 Antibacterial activity test of biosynthesized AuNPs.	39
4.10 Cytotoxicity effects of the biosynthesized AuNPs.	41
4.11 Microscopic images of 4T1, HepG2 and HDFa cells after the exposure of synthesized AuNPs (5 µg/ml) for 24 h.	42
4.12 UV-visible absorption of the concentrations of AuNPs.	43
4.13 The effect of the synthesized AuNPs on hatching rate of zebrafish embryos.....	43
4.14 Development of zebrafish embryos during 3 days of AuNPs exposure.	44

LIST OF ABBREVIATIONS

AuNPs	= Gold nanoparticles
cfu/ml	= Colony-forming unit per milliliter
cm	= Centimeter
CT	= Computed tomography
°C	= Degree Celcius
DMSO	= Dimethyl sulfoxide
DNA	= Deoxyribonucleic acid
EDXRF	= Energy Dispersive X-ray Fluorescence
FTIR	= Fourier transform infrared spectroscopy
h	= Hour
hpf	= Hour post fertilization
HAuCl ₄	= Tetrachloroauric acid
L	= Liter
M	= Molar
min	= Minute
ml	= Milliliter
mm	= Millimeter
mM	= Millimolar
nm	= Nanometer
µg	= Microgram

LIST OF ABBREVIATIONS (Continued)

μm	= Micromolar
μl	= Microliter
MRI	= Magnetic resonance imaging
MTT	= 3-(4,5-dimethylthiazol-2-yl)-2,5-diphenyltetrazolium bromide
NaBH_4	= Sodium borohydride
NaOH	= Sodium hydroxide
PBS	= Phosphate-buffered saline
PET	= Positron emission tomography
Rpm	= Revolutions per minute
TEM	= Transmission electron microscope
TISTR	= Thailand Institute of Scientific and Technological Research
SEM	= Scanning electron microscope
S.E.M	= Standard error of the mean
UV-Vis	= Ultraviolet-visible
XRD	= X-ray diffraction
<	= Less than
%	= percent
/	= Per

CHAPTER I

INTRODUCTION

1.1 Background/Problem

Gold nanoparticles (AuNPs) are currently one of the most promising research fields due to their unique properties such as large surface area and high dispersion, catalytic, optical, magnetic, electrical properties, biocompatibility, and non-toxicity (Yiing Yee, Periasamy, and Abd Malek, 2014). They have been gaining more interest and increasingly applied in many areas, especially in medicine and biology such as, biosensor, immune-analysis, detection and photo-thermolysis of microorganisms and cancer cells, optical bio-imaging, and drug delivery (Dykman and Khlebtsov, 2011).

In general, nanoparticles can be synthesized by using chemical or biological methods. Manufacturing processes in the chemical synthesis method can create some wastes containing toxic chemicals which are hazardous to people and the environment. In contrast, biological or green synthesis method which is a non-toxic, economical and environmentally friendly method is a better alternative method for AuNPs synthesis. Biosynthesis using plants has been successfully proven that it can be used to produce AuNPs. Green synthesis of AuNPs has been reported since the early 1900s (Mittal, Chisti, and Banerjee, 2013). Some bioorganic compounds from plants such as flavonoids, terpenoids, proteins, reducing sugars and alkaloids can be used as either reducing or capping agents during the formation of nanoparticles. The concentration of

these phyto-chemical compounds is critical in the shape and size directing process (Zhou et al., 2010). Crude extracts from several plants have been reported to be used as reducing agents in synthesis of AuNPs. In this study, green synthesis method was used to produce AuNPs using rhizomes of *Curcuma xanthorrhiza*, a spice plant grown in Indonesia. The characterization of the synthesized AuNPs were performed by UV-visible spectroscopy, X-ray diffraction (XRD), scanning electron microscope (SEM), Fourier transform infrared spectroscopy (FTIR), particle size analysis, energy dispersive X-ray fluorescence (EDXRF) and transmission electron microscope (TEM).

It has been reported that both AuNPs and AuNPs conjugated with antibiotics potentially improve bioavailability and increase target specificity of antibacterial agents (Mocan, 2013). AuNPs capped with dextrose produced bacteriostatic and bactericidal activities against both Gram-positive and Gram-negative bacteria. It was concluded that the efficiency of antibacterial activity was directly proportional to the increase in size of AuNPs (Badwaik et al., 2012). From disc diffusion method, the efficiency of antibiotic conjugated AuNPs gave higher inhibitory zone when compared to free antibiotics against all the three strains of *Escherichia coli*, *Micrococcus luteus* and *Staphylococcus aureus* (Saha et al., 2007). Moreover, polygonal AuNPs attached with vancomycin were generated and tested which showed that it effectively inhibited growth of pathogenic bacteria, including Gram-positive bacteria, Gram-negative bacteria and antibiotic-resistant bacteria, after illuminating with NIR light (Huang, Tsai, and Chen, 2007). Taken together, in this work antibacterial activity of AuNPs generated using rhizomes extract of *C. xanthorrhiza* was investigated in Gram-positive bacteria and Gram-negative bacteria.

Currently, organic dyes that widely used in textile and dyestuff industries for esthetic purposes has been a major concern as severe environmental pollution due to their undesirable effect to human and recalcitrance to treat. Because of their stability and complex atomic structure, the conventional techniques such as flocculation, membrane separation and ultrafiltration are not effective to decolorize or degrade these dyes. It has been reported that gold nanoparticle can be used as catalytic agents for degradation of some organic dyes (Joseph and Mathew, 2015). Therefore, in the present study, an evaluation of the catalytic potential of the synthesized AuNPs using *C. xanthorrhiza* to reduce the very toxic and non-biodegradable diazo dye Congo red in the presence of sodium borohydride (NaBH_4) was carried out.

With rapidly increasing applications of AuNPs in medicine such as bio-sensing, bio-imaging, catalysis, drug and gene delivery and photothermal-chemotherapy, researchers have highly concerned about their potential toxicities. However, *in vitro* toxicity study, the toxicity caused by AuNPs is still under debate due to the ambiguity in the studies undertaken to determine its safety (Shah et al., 2014). Some studies reported that AuNPs were non-toxic. Based on MTT assay, gold nanospheres capped with citrate, cysteine, glucose, biotin, and cetyltrimethyl-ammonium bromide (diameter of 4, 12, and 18 nm) were found to be non-toxic to human leukemia cells (Connor, Mwamuka, Gole, Murphy, and Wyatt, 2005). Similarly, AuNPs with the size of 3.5 nm in diameter that entered RAW 264.7 macrophage cells by endocytosis reduced the level of reactive oxygen species but did not induce any toxicity to the cells (Shukla et al., 2005). It was also found that citrate-capped AuNPs (10 nm in diameter) on dendritic cells could cause non-cytotoxicity, did not induce activation, and did not change the phenotype of the cells (Villiers, Freitas, Couderc, Villiers, and Marche, 2010).

However, other studies controversially reported that AuNPs are toxic. Both AuNPs and citrate-capped AuNPs have been reported that at the same dose, they were toxic to a human carcinoma lung cell line but not to human liver carcinoma cell line (Alkilany and Murphy, 2010). Moreover, gold nanospheres (1.4 nm diameter) was shown to cause mitochondrial damage, trigger necrosis, and induce an oxidative stress on HeLa cell lines (Pan et al., 2009). To assure that green biosynthesis of AuNPs using *C. xanthorrhiza* from this study is biocompatible, *in vitro* toxicity test was conducted in HepG2 (liver hepatocellular carcinoma), 4T1 breast cancer, and Human Dermal Fibroblast, adult (HDFa) cells.

In the past, *in vitro* and *in vivo* adverse effects of AuNPs from different types of synthesis have been intensively investigated (Khlebtsov and Dykman, 2011). Studies of biodistribution, accumulation and disposal in animals have also been reported (Lasagna-Reeves et al., 2010). However, data of toxicity on zebrafish development is quite limited. So the acute toxicity test of green synthesized gold nanoparticles in zebrafish embryos was included in the present study as well.

Herein, *C. xanthorrhiza* rhizomes were proven to be a good candidate for the biosynthesis of AuNPs. Biocompatibility of AuNPs, which is necessary for utilization in biomedical applications, such as catalytic agent, was confirmed to assure the safety of this green synthetic AuNPs product. This study provided additional evidence to support utilization of *C. xanthorrhiza*, a wide available Indonesian medicinal plant, with low cost and ease of AuNP biosynthesis.

1.2 Research objectives

1.2.1 To synthesize and characterize AuNPs using *C. xanthorrhiza* rhizomes.

1.2.2 To examine catalytic activity

1.2.3 To examine antibacterial activity of AuNPs

1.2.4 To determine their cytotoxicity and effects on the animal development in embryo of zebrafish.

1.3 Research hypothesis

The extract of *C. xanthorrhiza* rhizomes can be used to synthesize biocompatible AuNPs which possesses catalytic activity for degradation azo dye of Congo red and produces antibacterial effects against the tested bacteria.

1.4 Scope and limitation of the study

In this work, AuNPs were synthesized using *C. xanthorrhiza* and characterized. Their toxicity, catalytic and antimicrobial activity were evaluated. Catalytic activity was tested with only one dye, whereas antimicrobial effect was conducted with 4 species of bacteria. Three cell lines, Human hepatoma HepG2, 4T1 breast cancer and fibroblast cells, were used for *in vitro* toxicity test, while zebrafish was used for *in vivo* toxicity test.

CHAPTER II

LITERATURE REVIEW

2.1 Study of AuNPs

Gold have been used in medicine at least several thousand years ago. Colloidal gold was studied and used in alchemist laboratories during the Middle Ages in Europe. To date nanotechnology is the trending topic in all fields of scientific interest in the entire world and have already become key R and D (research and development) especially in Europe and North America (Aguar Fernandez and Hullmann, 2007). This is also evidenced by the exponential growth of research articles in the area of nanotechnology since 2001 to 2012 (Figure 2.1) (Shah et al., 2014).

Many applications of AuNPs have been developed such as drug delivery, catalysis, biosensing, imaging, etc. Gold nanoparticles have potential in drug delivery as well. Previous study demonstrated nitric oxide and singlet oxygen can be released by AuNPs. AuNPs also have ability in delivering large biomolecules such as peptides, proteins, or nucleic acids (Ghosh, Han, De, Kim, and Rotello, 2008).

AuNPs have been also found to act as a catalyst. They can catalyze selective reaction at low temperature but depend on the size and shape of AuNPs. AuNPs with diameters of about 5 or lower can be very effective catalysts (Hvolbæk et al., 2007). Because the small size of AuNPs increases the surface area, the catalytic active sites on the metal surface are readily available to incoming reagents (Prasad, Stoeva, Sorensen, Zaikovski, and Klabunde, 2003)

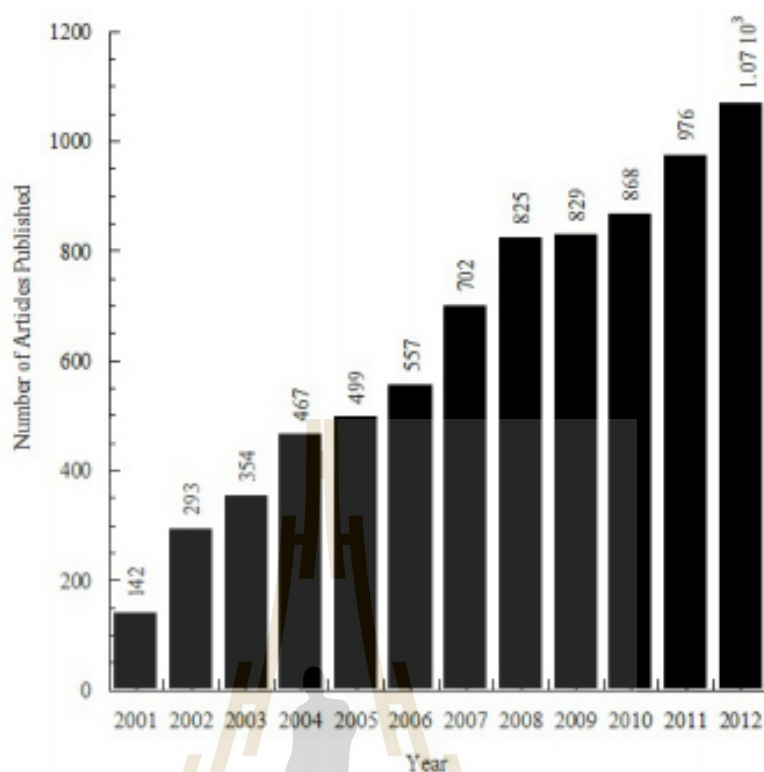


Figure 2.1 The number of articles published on nanoparticles since 2001-2012 (Shah et al., 2014).

For the application in biosensor, AuNPs can be used as a detector in chemical and biological samples. In chemical sample, AuNPs can be used to detect toxic ion (such as arsenic, mercury, antimony and chromium), carbon monoxide, nitric oxide, hydrazine, and various pesticides. Pesticides in drinking water at low concentration can also be detect by salt-induced aggregation of AuNPs (Gan and Li, 2012). In biological samples, it can be used to detect immunoglobulins, biomarker for cancer, small organic molecules, oligonucleotide, and proteins (Saha, Agasti, Kim, Li, and Rotello, 2012). AuNPs have been used for “First Response” kit in Carter-Wallace home pregnancy to detect hormone of pregnant women, by mixing the latex microparticles and AuNPs derivatized with a hormone released by pregnant women, causing the micro- and

nanoparticles coagulated in pink-colored clumps (Gan and Li, 2012). AuNPs also capable to detect DNA by modification of AuNPs with ss-DNA probes and introduced into a solution containing target ss-DNA. Then the particles will be aggregated when the target DNA contains the complementary base sequence to the probes resulting in color change of the colloidal solution (Nguyen, Kim, and Kim, 2011).

The high biocompatibility and versatile surface properties of AuNPs allow them to be used in modern imaging technique in medical imaging such as ultrasound (US), magnetic resonance imaging (MRI), computed tomography (CT), positron emission tomography (PET), PET/CT, and PET-MRI. CT imaging was used to detect tumor in a mouse model by intravenously injection of AuNPs, and after 4 h post injection the tumor was visible up by found most particles accumulated in the liver and bladder (Mahan and Doiron, 2018).

With the growing interest in the applications of AuNPs, the potential toxicity of AuNPs appears to be multi-faceted and difficult to predict. Previous study confirmed that generally AuNPs are non-toxic (Fratoddi, Venditti, Cametti, and Russo, 2015). Similarly, when AuNPs tested in the aquatic organisms, such as *Scenedesmus subspicatus*, *Daphnia magna* and *Brachydanio rerio*. The results showed that no mortality was observed at the concentration of 9.6 nM (≈ 100 mg/l) in the *Daphnia* test, at 1.9 nM (≈ 20 mg/l) in the fish test, and at 0.96 nM (≈ 10 mg/l) in the algae test (García-Camero et al., 2013).

2.2 Method for AuNPs synthesis

Principally AuNPs can be synthesized by two techniques: “bottom-up” and “top-down” (Figure 2.2). Bottom-up technique is a technique which formation of AuNPs

originates from individual molecules (Zhao, Li, and Astruc, 2013). This method consists of templating (Hall, Shenton, Engelhardt, and Mann, 2001), sonochemical (Okitsu, Ashokkumar, and Grieser, 2005), thermal reduction techniques (Magnusson, Deppert, Malm, Bovin, and Samuelson, 1999), and nanosphere lithography, chemical, photochemical, electrochemical (Pileni, 1997). Whereas, top-down technique, a bulk state Au is systematically broken down to generate AuNPs of desired dimensions. Photolithography (Sun et al., 2006), and electron beam lithography belong to this kind techniques (Schaal et al., 2012). Each method has their own drawbacks. Top-down approaches are generally quite expensive and resource-consuming. On the other hand, the bottom-up techniques are generally cheaper and better fit for large scale applications. Some of the more commonly used techniques in bottom up method for making AuNPs are discussed in the following sections.

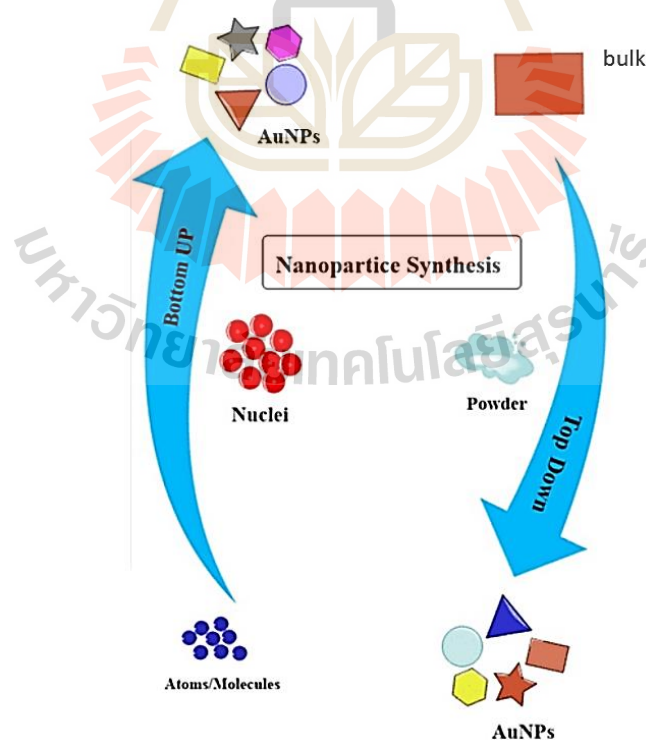


Figure 2.2 Technique for synthesis of nanoparticles (Ahmed, Annu, Ikram, and Yudha S, 2016).

2.2.1 Turkevich method

The Turkevich method was first described by J. Turkevich et al. in 1951. The principle of this method is reduction of gold ions (Au^{3+}) to gold atoms (Au^0) which needs reducing agents like citrate, amino acids, ascorbic acid or UV light (Shah et al., 2014). Figure 2.3 is an example of the synthesis mechanism of gold nanoparticles using citrate reduction method according to Turkevich method. The AuNPs formation observed experimentally at different reaction conditions can be interpreted as a four step. The initial stage is nucleation step, a rapid formation of nuclei (step a in Figure 2.3) followed by coalescence of the nuclei into bigger particles (step b in Figure 2.3). The third step consists of slow diffusion growth of particles sustained by ongoing reduction of gold precursor as well as a further coalescence (step c in Figure 2.3). Following that, particles grow rapidly to their final size which imposed by complete consumption of the precursor species (step d in Figure 2.3).

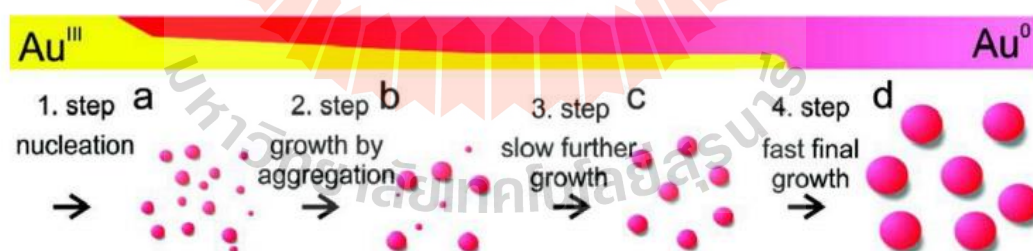


Figure 2.3 Illustration of the synthesis mechanism of AuNPs using citrate reduction method according to Turkevich method (Shah et al., 2014).

2.2.2 Brust method

Brust method was established by Brust and Schiffrin in 1994. Figure 2.4 is the synthetic steps involved in the Brust synthesis of gold nanoparticles. Briefly, HAuCl_4 is transferred to an organic phase (usually toluene) through tetraoctyl ammonium bromide (TOAB). The Au^{3+} to Au^0 reduction is performed by adding an aqueous solution of NaBH_4 to the same reaction mixture, resulting in a color change of the reaction from orange to brown (Shah et al., 2014).

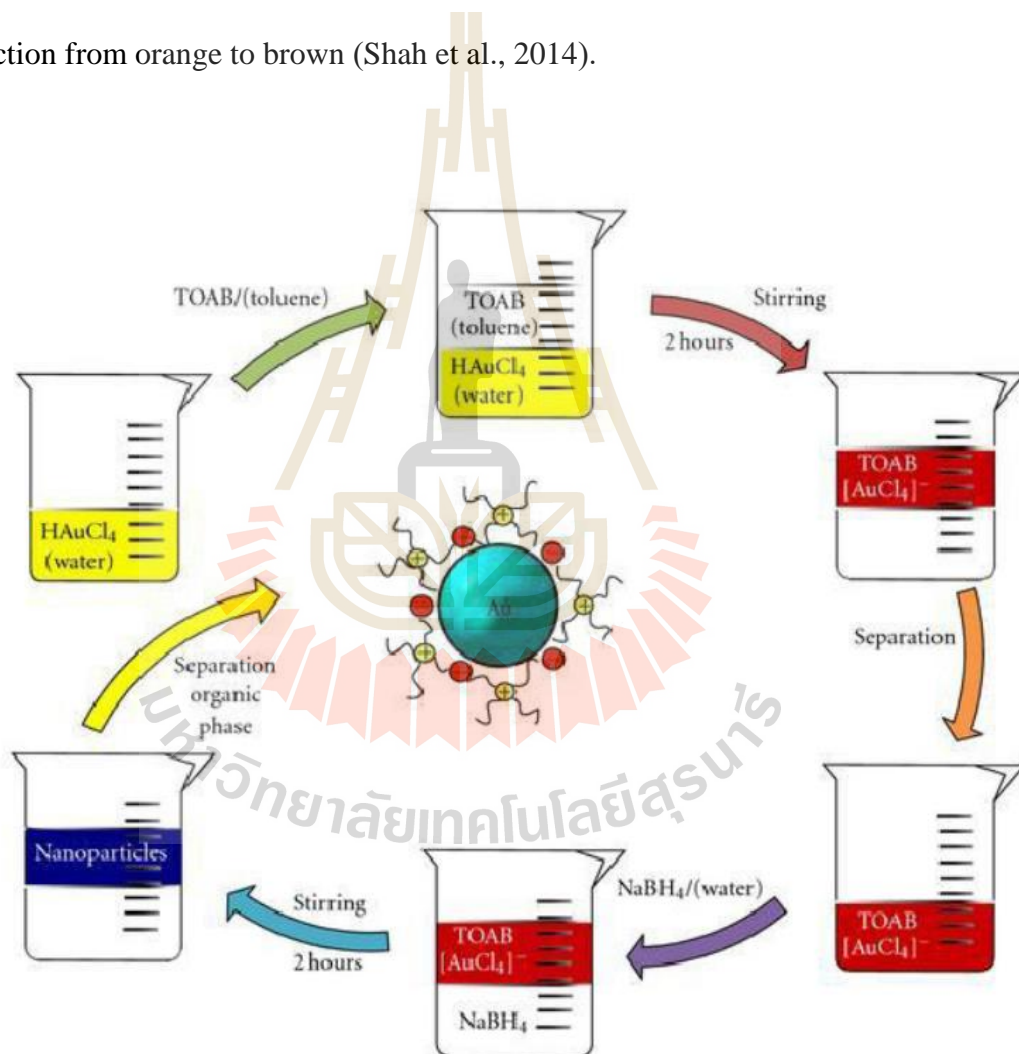


Figure 2.4 The synthetic steps involved in the Brust synthesis of AuNPs (Shah et al., 2014).

2.2.3 Seeded growth method

Seeded growth method is described in Figure 2.5. Basically, the principle of this method is to first produce seed particles by reducing HAuCl_4 with a strong reducing agent (e.g sodium borohydride). In the second step, the seed particles are added to a solution of metal salt in presence of a weak reducing agent like ascorbic acid and structure directing agent to prevent further nucleation, thus resulting accelerate the anisotropic growth of AuNPs (Zhao et al., 2013).

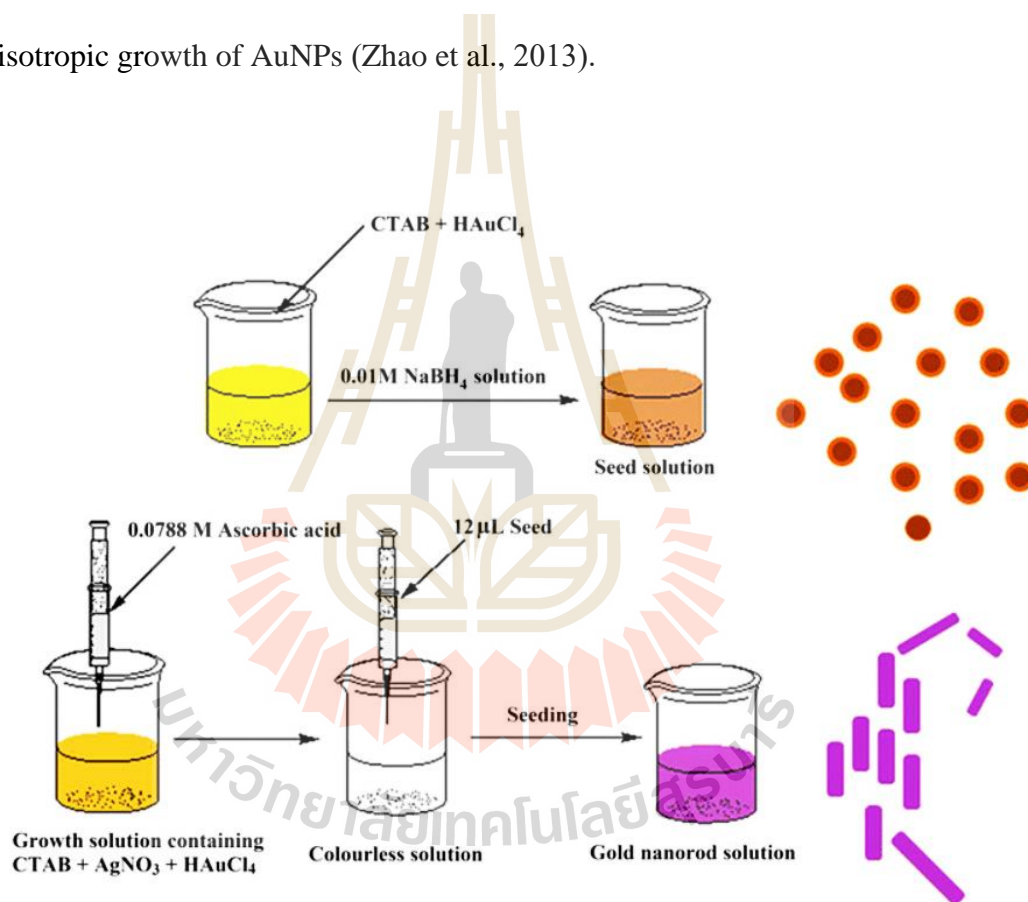


Figure 2.5 Scheme of seeded growth method for synthesizing AuNPs (Sharma et al., 2015).

2.2.4 Biological synthesis by plant constituents

Synthesis of metallic nanoparticles using plant constituents has been shown to produce nanoparticles with shapes and sizes that are comparable with those produced

through chemical and physical methods (Parsons, peralta-vidya, and Gardea-Torresdey, 2007). Various bio-components from plants such as flavonoids, phytosterols, quinones etc. are required in synthesis of AuNPs as they possess functional groups which catalyze the reduction and stabilization of AuNPs (Shah et al., 2014).

Figure 2.6 shows the scheme of biological synthesis by plant constituents. The procedure is simple by mixing plant constituents with HAuCl_4 salts for definite amount of time. This process does not require to add external stabilizing/capping agents, because phytochemicals itself acts as reducing as well as stabilizing agents (Ahmed, Annu, Ikram, and Yudha S, 2016). In this method, pH, temperature, reaction time and dosage of biomass are important factors that have a relationship with the size and shape of nanoparticles (Gan and Li, 2012). Some studies of AuNPs synthesis using plants is summarized in Table 2.1.

2.2.5 Synthesis method using microorganisms

Biosynthesis of AuNPs also can be produced by using microorganisms such as bacteria (Klaus-Joerger, Joerger, Olsson, and Granqvist, 2001), fungi (Sastry, Ahmad, Islam Khan, and Kumar, 2003), and yeast (Pimprikar, Joshi, Kumar, Zinjarde, and Kulkarni, 2009). AuNPs can be produced using this method by two ways, namely, extracellular and intracellular productions. For the extracellular production, Au^{3+} is reduced by the cell wall reducing enzymes or soluble secreted enzymes. While, the reduction of intracellular production occurs inside the cell. Microbial cells are isolated and purified using various techniques which are then treated with gold salts to obtain AuNPs (Zhao et al., 2013).

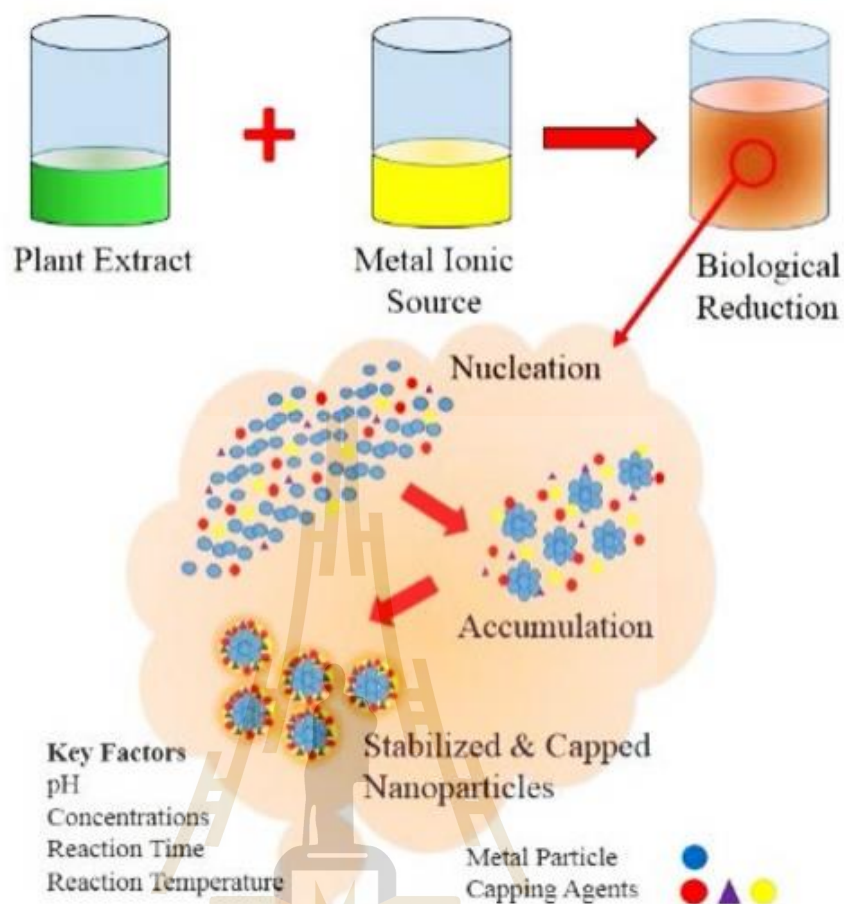


Figure 2.6 Biological synthesis by plant constituents (Monaliben Shah, Fawcett, Sharma, Tripathy, and Poinern, 2015).

2.2.6 Synthesis method using bio-molecules

Bio-molecules are defined as molecules produced by living organisms that have biological functions in the body. Amino acids, nucleic acids, carbohydrates and lipids are member of bio-molecules, that possess hydroxyl and carbonyl functional groups which can reduce Au^{3+} ions to Au^0 neutral atoms. Au^0 are then capped to form stabilized AuNPs (Shah et al., 2014).

Table 2.1 Biosynthesis of AuNPs by using extract from part of plant.

No.	Plant as bioreductant	Shape	Size (nm)
1	<i>Cymbopogon citrates</i>	Spherical, triangular, hexagonal, and rod shapes	20-50
2	<i>Syzygium cumin</i>	Spherical	10-15
3	<i>Abelmoschus esculentus</i>	Spherical	45-75
4	<i>Trianthema decandra L</i>	Spherical, cubical and hexagonal	37.7-79.9
5	<i>Cassia auriculata</i>	Triangular and spherical	15-25
6	<i>Stevia rebaudiana</i>	Spherical	2 and 50
7	<i>Grape waste</i>	Spherical	20-25
8	<i>Hovenia dulci</i>	Spherical and hexagonal	20
9	<i>Barbated Skullcup</i>	Spherical	5-30
10	<i>Psidium guajava</i>	Spherical	4-24
11	<i>Syzygium aromaticum</i>	Irregular	5-100
12	<i>Banana peel extract</i>	-	300
13	<i>Mentha piperita</i>	Spherical	90
14	<i>Maduca longifolia</i>	Triangular	Variable
15	<i>Solanum torvum</i>	Spherical	1-100
16	<i>Dysosma pleiantha</i>	Spherical	127
17	<i>Gymnema sylvestre R. Br</i>	Spherical	50
18	<i>Tagetes patula</i>	Spherical	45
19	Palm oil mill effluent	Spherical	18.75 ± 5.96
20	<i>Stevia rebaudiana</i>	Spherical	5-20

Source: (Shah et al., 2014).

2.3 Biosynthesis mechanism of metal nanoparticles

The mechanism for the metal nanoparticles formation is shown schematically in Figure 2.7, where a three-step process has been determined. The first step of the process is the activation phase, which is the reduction of metal ions and nucleation of the reduced metal atoms occur. The following step is the growth phase, which is the small adjacent nanoparticles spontaneously coalesce into particles of a larger size (direct formation of nanoparticles by means of heterogeneous nucleation and growth, and further metal ion reduction; a process referred to as Ostwald ripening); and the last is the process termination phase determining the final shape of the nanoparticles.

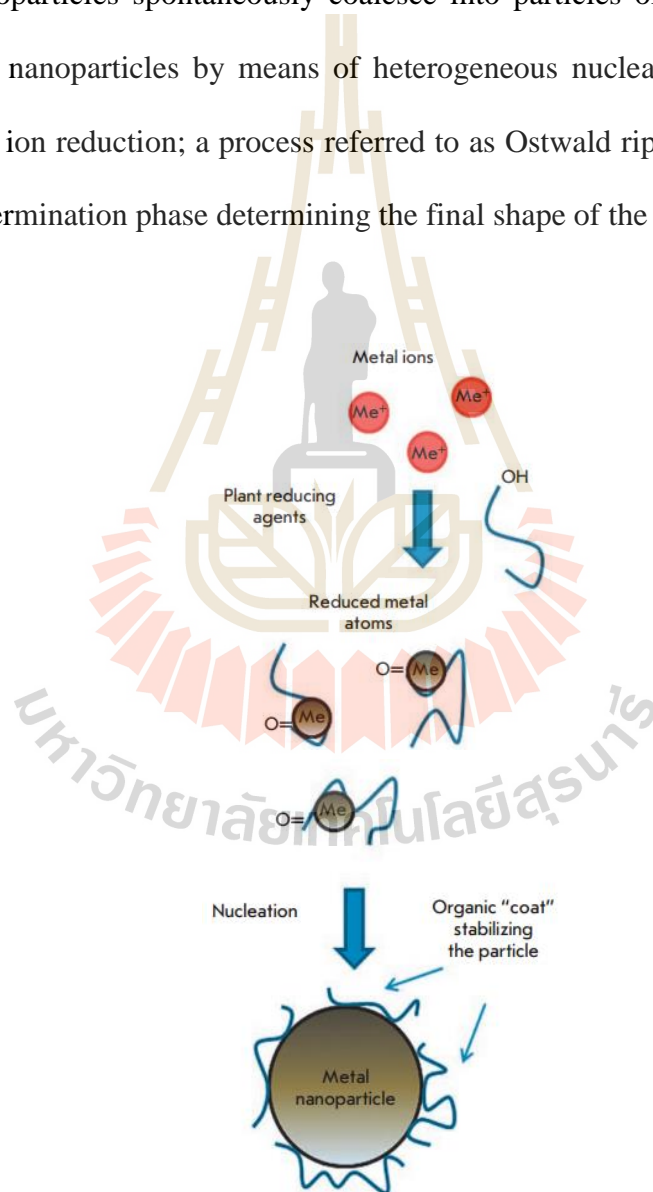


Figure 2.7 Mechanism of metal nanoparticle synthesis in plants (Makarov et al., 2014).

2.4 *Curcuma xanthorrhiza*

C. xanthorrhiza (Figure 2.8), which was used as reducing agent to synthesize AuNPs in this study, is a member of Zingiberaceae that originate from Indonesia. It is an herb plant with height more than 1 m and less than 2 m. Its flower is yellow; rhizomes are reddish brown, dark yellow or dark green and branched. The rhizomes of *C. xanthorrhiza* comprise volatile oil, saponin, flavonoid and tannin. The major components of its rhizomes are starch (48.18-59.64%), fiber (2.58-4.83%), volatile oil (1.48-1.63%) (such as phelandren, camphor, tumerol, sineol, borneol, and xanthorrhizol, and curcuminoids such as curcumine and desmetoxicurcumine (1.6-2.2%) (Mangunwardoyo, 2012). Curcumin is commonly used as flavoring and coloring agent, food preservative, and a spice (Bhawana, Basniwal, Buttar, Jain, and Jain, 2011). In Indonesia, this plant is used as supplement health or as traditional medicine for many diseases such as hepatitis, liver complaints, diabetes, rheumatism, anticancer, hypertension, and heart disorders (Salleh, Ismail, and Ab Halim, 2016). The main active ingredient curcumin is soluble in ethanol, alkalis, ketone, acetic acid and chloroform; but is insoluble in water (Araujo and Leon, 2001). Chemically, curcumin is a diarylheptanoid (terpenoids) which is also found in *Curcuma manga*. It has been reported that it is responsible for reducing the Au^{3+} to Au^0 . The reduction of Au^{3+} to Au^0 induces the formation of nuclei, and then these nuclei coalesce and contribute to the growth of AuNPs. Another terpenoids with carboxylic groups such as Longpene A, Coronadiene, and Zerumin A can bind to AuNP surfaces and act as a stabilizing agent (Foo, Periasamy, Kiew, Kumar, and Malek, 2017).



Scientific classification of

C. xanthorrhiza:

Kingdom	: Plantae
Clade	: Angiosperms
Order	: Zingiberales
Family	: Zingiberaceae
Genus	: <i>Curcuma</i>
Species	: <i>C. xanthorrhiza</i>

Figure 2.8 *C. xanthorrhiza* rhizomes.

2.5 Cytotoxicity effect of AuNPs

Several studies have been reported the effects of AuNPs (capped or uncapped) on the cells. Effects of nanoparticles on a cellular level can occur by interacting with membrane, mitochondria or nucleus causing organelle or DNA damage, oxidative stress, apoptosis (programmed cell death), mutagenesis, and protein up/down regulation (Alkilany and Murphy, 2010).

AuNPs capped with either sodium citrate or polyamidoamine dendrimers have been shown to exhibit *in vitro* genotoxicity and cytotoxicity even at very low concentrations. Peripheral blood mononuclear cells appear to be less sensitive to DNA damage toxicity effects than cancer HepG2 cells upon exposure to AuNPs (Paino, Marangoni, de Oliveira Rde, Antunes, and Zucolotto, 2012). Similar results were obtained on the biosynthesis of AuNPs using the seed coat of *Cajanus cajan* which led to HepG2 cell apoptosis with spherical shapes of AuNPs having the size of 9 to 41 nm

in diameter (Ashokkumar et al., 2014). Uncapped AuNPs with nano-rod structure and average particle size at 10-40 nm induced cell death (human normal lung fibroblast, mouse embryonic fibroblast and African green monkey kidney cells) at various dose (Chueh, Liang, Lee, Zeng, and Chuang, 2014). In contrast to these results, another study explained that AuNPs coatings with citrate and 11-mercaptopundecanoic acid did not induce significant cytotoxicity in human liver HepG2 cells (Fraga et al., 2013).

As described above, toxicity reports of gold nanoparticle are controversial. It has been suggested that cytotoxicity effect of AuNPs depend on the dose or size of AuNPs. The study of cytotoxic effects of AuNPs in six of mammalian cell lines induces a dose-dependent suppression of cell growth with different levels of severity and the suppressive effect of AuNPs was indirectly associated with their sizes and cellular uptake (Chuang et al., 2013). Similarly, the small particle size of AuNPs (5 nm diameter) were more toxic to human neural precursor cells compared to large particle size (100 nm diameter) (Lee, Yoo, Kim, and Yoo, 2016).

It has been demonstrated that the extracellular synthesized AuNPs using culture supernatant of *Enterococcus sp.* increased cytotoxicity activity against HepG2 and lung cancer (A549) cells in concentration-dependent manner (Rajeshkumar, 2016). Moreover, by using colony forming efficiency assay, the effect of AuNPs on Balb/3T3 mouse fibroblasts was found to be toxic only with 5 nm diameter of AuNPs, while no cytotoxic effects were seen in the cells exposed to 15 nm size of AuNPs for 72 h at concentration higher than 50 μ M (Coradeghini et al., 2013). A study using green synthesis method by *Areca catechu* nut found that the synthesized AuNPs caused 66% death of HeLa cells at 100 μ g/ml (Rajan, Vilas, and Philip, 2015). Nevertheless, other

reports explained that AuNPs were not toxic to any of the cells. For example, AuNPs were not toxic to Balb/c 3T3 fibroblasts, NR8383 macrophages, and U937 monocytes with particle size 13 ± 1 nm and the concentrations up to $6.0 \mu\text{g/ml}$ (Mannerstrom, Zou, Toimela, Pyykko, and Heinonen, 2016). Similarly, gallic acid capped AuNPs were not lethal to the mouse embryonic fibroblasts cells at 100 ppm (Kim, Kim, Shinde, Sung, and Ghodake, 2017). Therefore, toxicity of gold nanoparticle remains unclear and needs further investigation.

2.6 Zebrafish model

Zebrafish is becoming popular in the field of toxicology and biomedical research, due to their small size, very high reproducibility (Chakraborty, Sharma, Sharma, and Lee, 2016), quick development (Truong, Saili, Miller, Hutchison, and Tanguay, 2012), and transparency of the embryo (Ganeshkumar et al., 2012). On the other hand, zebrafish is a complete animal model to examine the nanoparticles toxicity because the organs system such as cardiovascular, nervous and digestive systems of this model animal are like mammal (Chakraborty et al., 2016).

Zebrafish has four stages of development as demonstrated in Figure 2.9. The initial stage is an embryo growth from the one-cell stage (0 h post-fertilization) to the mid-somitogenesis stage (~ 18 h post-fertilization). In this state, the trunk musculature can be clearly seen in the “chevron-shaped” somites. The following stage is the most axial patterning (head, trunk, and tail) which is completed in 24 h. The third stage is the larvae which occurs during day 2 of development, and the larvae start to take food on day 5. Then, after 3 weeks of development, some metamorphosis takes place, including

thickening of the skin, development of scales and sex differentiation, and the larvae completed to be an adult (Pyati, Look, and Hammerschmidt, 2007).

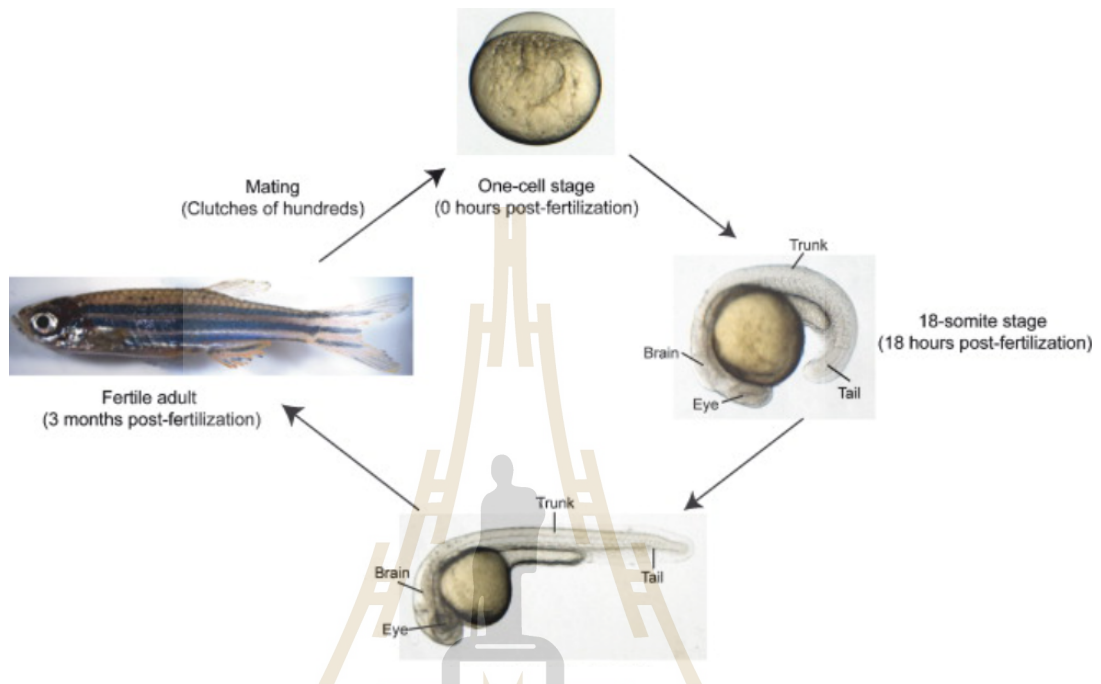


Figure 2.9 Zebrafish life cycle (Pyati et al., 2007).

As performing toxicity experiments on human are ethical problems, biomedical research to study drug toxicity has mostly conducted in small mammal model, usually rats and mice, because many biologic processes between humans and lower vertebrates are relatively conserved. Although these models have significant advantages, they are also expensive to maintain and difficult to manipulate embryonically. The zebrafish model is chosen to test the developmental toxicity of AuNPs in this study instead.

2.7 Antibacterial activity of AuNPs

2.7.1 Antibacterial studies of AuNPs

Many reports demonstrated that AuNPs exhibited antibacterial effects against several pathogen bacteria, such as *S. aureus*, *Bacillus subtilis*, *B. cereus*, *E. coli*, *Pseudomonas aeruginosa*, *Proteus vulgaris*, however, some studies showed no antibacterial activity. Several studies on antibacterial activity of AuNPs have been published, where some of them are summarized in Table 2.2.

2.7.2 The mechanism of nanoparticles toxicity against bacteria

The specific mechanism of nanoparticles toxicity against bacteria are not understood completely. Some study explained that nanoparticles can attach to the membrane of the bacteria by electrostatic interaction and disrupt the integrity of the bacterial membrane. However, the mechanism of nanoparticles toxicity depends on composition, surface modification, intrinsic properties and the bacterial species (Hajipour et al., 2012). Figure 2.10 describes possible mechanism of bactericidal action of AuNPs on *E. coli*.

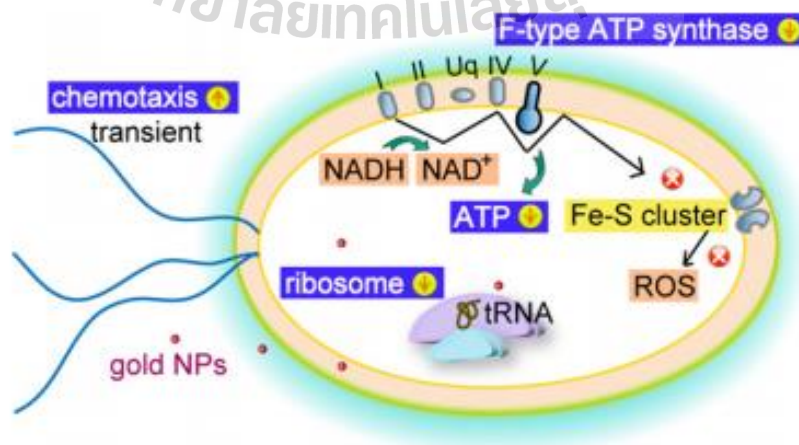


Figure 2.10 The bactericidal illustration of AuNPs on *E. coli* (Cui et al., 2012).

Table 2.2 Antibacterial agents of biosynthesis of AuNPs.

Bacteria species	Size of AuNPs (nm)	Bio-reduction	The effect	Reference
<i>E. coli</i> and <i>B. subtilis</i>	40	<i>Rhazya stricta decne</i>	against <i>E. coli</i> and <i>B. subtilis</i> at 25 µg/ml and 50 µg/ml, respectively.	(Ahmad et al., 2017).
<i>S. aureus</i> and <i>P. aeruginosa</i> .	16	<i>Ananas comosus</i>	against <i>S. aureus</i> and <i>P. aeruginosa</i> at the concentration of 50 µg/ml.	(Bindhu and Umadevi, 2014).
<i>P. aeruginosa</i> .	7-20	<i>Actinidia deliciosa</i> fruit	damaging the cell membrane of <i>P. aeruginosa</i> at 1.0 mM of AuNPs.	(Naraginti and Li, 2017).
<i>Pseudomonas syringae</i> , <i>E. coli</i> , and <i>Shigella sonnei</i> .	20-30	<i>Trichoderma viride</i>	inhibit the growth up to 53%, 47%, and 55% at concentration 500 mg/l for <i>E. coli</i> , <i>S. sonnei</i> and <i>P. syringae</i> , respectively.	(Mishra et al., 2014).
<i>S. aureus</i> , <i>B. subtilis</i> , <i>B. cereus</i> , <i>E. coli</i> , <i>P. aeruginosa</i> and <i>Proteus vulgaris</i> .	7.9-2.6	<i>Dracoccephalum kotschy</i> leaf	no antibacterial activity.	(Dorosti and Jamshidi, 2016).
<i>B. subtilis</i> and <i>E. coli</i> .	20	<i>Gloriosa superba</i> leaf	AuNPs did not showed toxicity.	(K. Gopinath et al., 2016).
<i>S. aureus</i> and <i>E. coli</i> .	5-25	<i>Parkia roxburghii</i> leaf	antibacterial activity against both types of bacteria at 1.0 mM of AuNPs.	(Paul, Bhuyan, Purkayastha, and Dhar, 2016).
<i>Shigella flexneri</i> , <i>Proteus mirabilis</i> , <i>B. cereus</i> and <i>B. subtilis</i> .	16-20	hydroxy ethyl starch and methylacrylate	no effect on <i>S. flexneri</i> and <i>P. mirabilis</i> , but inhibited <i>B. cereus</i> and <i>B. subtilis</i> at concentration 50 µg/ml.	(Das, Pandey, Pal, Kolya, and Tripathy, 2015).

CHAPTER III

MATERIALS AND METHODS

3.1 Plant preparation and extraction

C. xanthorrhiza rhizomes were purchased from the local market in Indonesia. Fresh plant rhizomes of *C. xanthorrhiza* were washed to remove the soil and mud from the outer skin. Cleaned rhizomes cut into small pieces and dried by hot air oven at 40°C for 7 days to remove the moisture. Then, dried plant was grounded into powder and kept in -20°C for further use.

The extraction was prepared from 40 mg of *C. xanthorrhiza* powder by adding 2 ml of 10 mM NaOH solution and the volume was made up to 10 ml by deionized water, then filtered with 0.45 µm membrane syringe filter. The extract was immediately used for the synthesis of AuNPs.

3.2 Synthesis and characterization of AuNPs

3.2.1 Synthesis

For the synthesis of AuNPs, 1 ml of 1 mM tetrachloroauric acid (HAuCl₄) was mixed with varying quantity (0.5, 1, 1.5, 2, and 2.5 ml) of *C. xanthorrhiza* extract with 10 ml final volume. The mixture was continuously stirred while *C. xanthorrhiza* extract is adding drop by drop and then left to stand at room temperature for 24 h. Surface plasmon resonance at 530-550 nm was monitored by UV-Visible spectroscopy for 24 h to ascertain the formation of nanoparticles.

The AuNPs colloidal were washed 3 times to remove unreacted chemicals by centrifugation at 14,000 rpm for 15 min with deionized water. Its concentration was measured by using the Beer's Law equation below.

$$\text{Absorbance} = \epsilon L c$$

where ϵ = molar absorptivity constant

L = the path length of the cell holder

c = concentration

3.2.2 Characterization

3.2.2.1 Ultraviolet-visible spectrophotometry

The reduction of HAuCl_4 to AuNPs by the extract of *C. xanthorrhiza* was monitored using ultraviolet-visible spectrophotometry (UV-Vis) at 1, 3, 6, 12, and 24 h. The absorption spectra were scanned at the wavelength of 300-700 nm (Thermo Scientific Multiskan GO, Finland).

3.2.2.2 Zeta potential measurement and particle size analysis

Zeta potential measurement and the average particle size distribution of biosynthesis AuNPs were recorded by using Zeta sizer (Malvern Instrument Ltd, USA). The average particle size distribution of biosynthesis AuNPs were recorded based on their intensity and volume respectively (Santhosh, Ragavendran, and Natarajan, 2015).

3.2.2.3 X-ray diffraction (XRD)

AuNPs colloids were prepared by the method mentioned in section 6.2.1 and lyophilized. The crystallinity of the synthesized AuNPs were analyzed by XRD (D2 Advance, Bruker, Germany) according to the method described previously (Geethalakshmi and Sarada, 2013).

3.2.2.4 Scanning electron microscopy (SEM)

Thin films of the sample were prepared on a carbon coated copper grid by dropping a very small amount of the sample on the grid. Extra solution was removed using a blotting paper and then the film on the SEM grid was air dried for a few minutes (Faramarzi and Forootanfar, 2011) and analyzed by SEM (Zeiss AURIGA FE-SEM/FIB/EDX machine: Jena, Germany).

3.2.2.5 Transmission electron microscopy (TEM) and energy dispersive X-ray fluorescence (EDXRF)

A drop of synthesized colloidal sample was deposited on a carbon coated copper grid followed by drying at 60°C. TEM (Model FEI Tecnai G2 20 200kV TEM/STEM/EDX/Tomography, USA) was used for analysis of the shape and size of nanoparticles (Shameli et al., 2012), while the purity and chemical composition were analyzed by EDXRF (Horiba XGT-5200 X-ray) (Santhosh et al., 2015).

3.2.2.6 Fourier transform infrared spectroscopy (FTIR)

The possible biomolecules responsible for reduction of the Au^{3+} to Au^0 was pursued by FTIR (Abdel-Raouf, Al-Enazi, and Ibraheem, 2017). Briefly, dried sample was prepared by the method mentioned in section 6.2.2.2. The powder was subjected to FTIR (RAM II FT-Raman, Bruker, Germany) and compared to *C. xanthorrhiza* rhizomes powder.

3.3 Examination of catalytic activity of the synthesized AuNPs

Freshly prepared NaBH_4 solution (0.2 M, 100 μl) was mixed with 3 ml of the azo-dye solution of Congo red (30 $\mu\text{g/ml}$), then 100 μl of AuNPs (Final concentration: 0.5 $\mu\text{g/ml}$). colloidal was added to the mixture. The reaction rates of Congo red

reduction with and without AuNPs were monitored by spectrophotometer at 300-700 nm at room temperature. The reaction mixture of Congo red and NaBH₄ was kept as control (Guo, Li, Yang, and Liu, 2015).

3.4 Antibacterial test

Bacteria used in this study was obtained from Thailand Institute of Scientific and Technological Research (TISTR). The antibacterial activities of AuNPs was evaluated against Gram-positive bacteria (*S. aureus* (TISTR 1466) and *B. cereus* (TISTR 687)) and Gram-negative bacteria (*E. coli* (TISTR 780) and *Enterobacter aerogenes* (TISTR 1540)). The screening of the antibacterial activity was performed using disc diffusion method (Humeera et al., 2013). Antibacterial test was analyzed by disc diffusion method. At first, a colony of Gram-positive and Gram-negative bacteria were cultured in Müller-Hinton broth (MHB) at 37°C and shaken at 200 rpm for 16 h. After 16 h, cell suspensions were inoculated on Müller-Hinton agar (MHA) and adjusted concentration equivalent to that of a 0.5 McFarland standard (~10⁸ cfu/ml) prior to swabbing down entire agar surface. AuNPs (60 µg) and extract (40 µg) were dropped onto circular sterile paper disc (5 mm in diameter of Whatman No. 1). These sterile filter papers were exposed to UV light for 30 min and then placed on the previously inoculated agar plate. After incubation for 24 h at 37°C, the clear zones of inhibition around the disks were observed and measured. (Kavita, Singh, and Jha, 2014). Ampicillin (10 µg) and kanamycin (10 µg) were used as positive controls for Gram-positive and Gram-negative bacteria, respectively (Khamhaengpol and Siri, 2016).

3.5 Cytotoxicity assay

3.5.1 MTT assay

HepG2, 4T1 breast cancer, and HDFa cells were used in cytotoxicity assay according to Rajeshkumar (2016) with some modifications. Concisely, 1×10^4 cells/well were seeded in 96 well plates and left overnight. Cells were treated with various concentrations (0-5 $\mu\text{g/ml}$) of gold nanoparticles and incubated for 24 h at 37°C. After washed with PBS, cells were added with MTT (0.5 mg/ml) and further incubated for 4 h. Then, MTT solution was removed and the crystals were then dissolved by adding 100 μl of DMSO. Absorbance of the purple blue of formazan dye was measured with spectrophotometer (Benchmark Plus Microplate Spectrophotometer from Bio-Rad, Japan) at a wavelength of 570 nm.

3.5.2 Trypan blue exclusion test

This method was performed using the method previously reported with minor modification (Chudapongse, Kamkhunthod, and Poompachee, 2010). HepG2, 4T1 breast cancer, and Fibroblast cells (1×10^4 cells/well) were seeded in 96 well plates overnight and then treated with AuNPs for 24 h with various concentrations (ranging from 0-5 $\mu\text{g/ml}$). After 24 h, cells were washed with PBS and harvest with 0.25% trypsin-EDTA solution at 37°C for 5 min. Cells were collected and centrifuged for 3 min, 1300 rpm (for HepG2 and HDFa cells) or 200 rcf (for 4T1 breast cancer), then resuspended with the RPMI 1640 and DMEM completed media, respectively. The cell suspension was mixed with an equal volume of trypan blue, which is for staining dead cells and unstaining viable cell. The cells were counted under a light microscope by using a hemocytometer.

3.6 Zebrafish embryo toxicity test

3.6.1 Zebrafish rearing

Zebrafish was reared in an aquarium that consisting of reverse osmosis water with photoperiod a 12 h light/ 12 h dark. They were fed twice daily of normal food and once daily of Artemia (Truong et al., 2012). All procedures in this study were approved and conducted according to guidelines of the Institutional Animal Care and Use Committee, Suranaree University of Technology under Associate Prof. Dr. Nuannoi Chudapong's Project (Toxicity study of nanomaterials using zebrafish model).

3.6.2 Exposure protocol

Prior to exposure, to produce embryos: two males and three females of zebrafish put in the breeding tank. Newly fertilized eggs of zebrafish, approximately 20 of 3 h post fertilization (hpf) were exposed to 2 ml of different concentration of AuNPs (0-5 $\mu\text{g/ml}$) for four days in 24-well plate. Distilled water was used as control. The mortality and malformations of zebrafish embryos at 96 hpf was used following the OECD guidelines (OECD, 2013).

3.7 Statistical analysis

Data was expressed as mean \pm S.E.M. Comparisons among different groups were performed by analysis of variance (ANOVA) followed by Student-Newman-Keuls test. *P*-values less than 0.05 was set as the level of significance.

CHAPTER IV

RESULTS

4.1 UV-vis spectrophotometry analysis

The AuNPs reaction was started after addition of *C. xanthorrhiza* rhizomes extract to 1 mM aqueous HAuCl₄, resulting in the color change from pale yellow to pink-ruby red in 30 min. The green synthesis of AuNPs was effectively performed using the *C. xanthorrhiza* rhizomes extract as both reducing and capping agent, and HAuCl₄ as the precursor. This method called as green synthesis due to no other hazardous or toxic chemicals were used in this synthesis process. It was monitored by UV-vis spectroscopy at wavelength 300-700 nm, which is usually the first technique to observe a collective excitation of the electrons in the conduction band around the nanoparticle surface. The color change indicates the formation of AuNPs in the solution. *C. xanthorrhiza* rhizomes extract without HAuCl₄ did not show any color changes or conversely. Figure 1 A shows the absorption spectra of AuNPs prepared using different concentrations of *C. xanthorrhiza* rhizomes extract. It was observed that when the amount of the extract was increased from 0.5-1.5 ml, the λ_{\max} shifted to a lower wavelength from 557 to 538 nm. Based on this data the optimal concentration of *C. xanthorrhiza* rhizomes extract for the highest yield with 1 ml of 1 mM HAuCl₄ was 1.5 ml. This optimal concentration was chosen for all of further experiments. Figure 1 B shows time-evolution monitored by UV-vis absorption. The optimal time at 24 h was chosen for further experiments throughout the study.

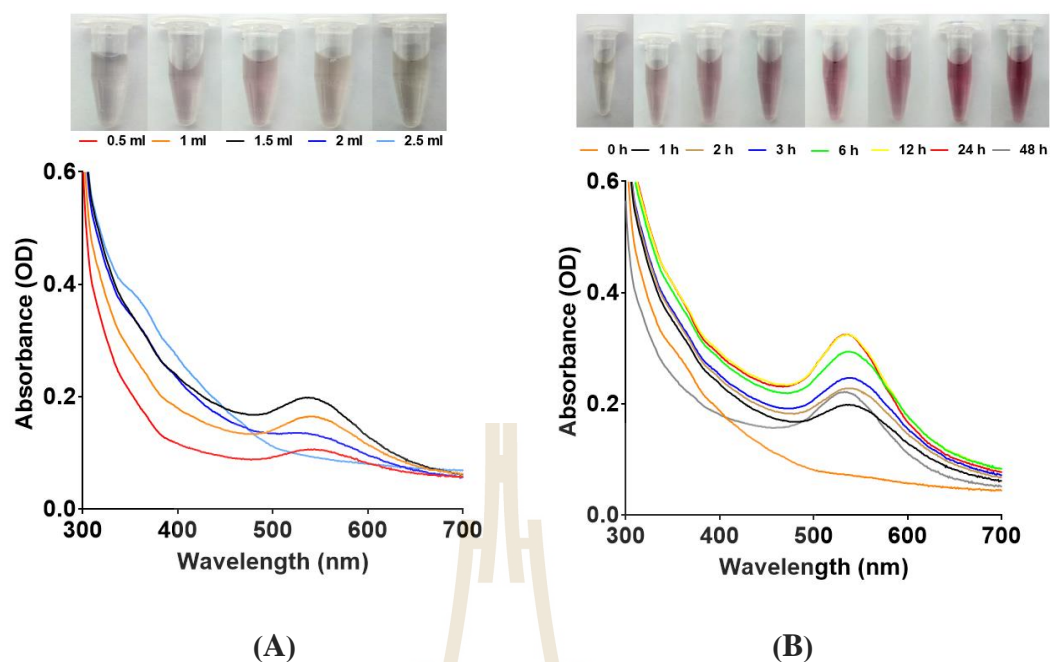


Figure 4.1 UV-visible absorption spectra of AuNPs synthesized by using *C. xanthorrhiza* rhizomes extract. Effect of different concentrations of rhizomes extract on biosynthesis of AuNPs at 1 h is shown in panel (A), whereas the time variation of the synthesis using 1.5 ml of the extract is in panel (B). Color change during the phyto-reduction of HAuCl_4 was noticeable as shown above the curves.

4.2 X-ray diffraction

Crystalline nano structure of biologically synthesized AuNPs was confirmed by XRD analysis. Figure 4.2 revealed that the characteristic diffraction peaks of AuNPs were located at $2\theta = 38.19^\circ, 44.39^\circ, 64.58^\circ, 77.57^\circ,$ and 81.73° which correspond to (111), (200), (220), (311), and (222) reflections of face centered cubic (FCC) structure of metallic gold from the range of 20-90, respectively. The mean size of AuNPs was calculated using the Debye–Scherrer’s equation by determining the width of the (1 1 1) Bragg’s reflection which was around 10 nm.

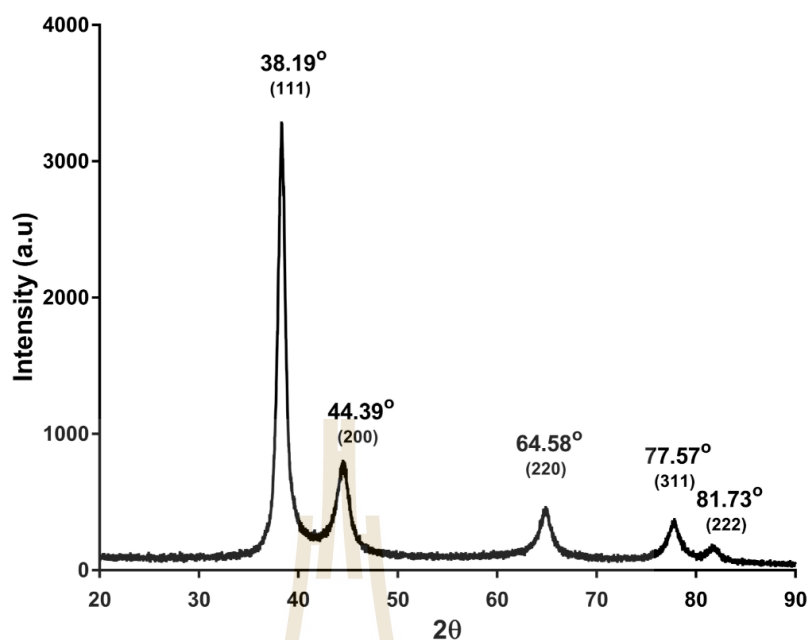


Figure 4.2 X-ray diffraction pattern of AuNPs obtained from 1.5 ml of *C. xanthorrhiza* rhizomes extract at 24 h.

4.3 SEM, TEM and EDXRF studies

Characterization of the morphology and size of AuNPs were carried out using SEM (Figure 4.3), and TEM (Figure 4.4A). Their corresponding particle size distribution histograms of the biosynthesized AuNPs from the TEM images is illustrated in Figure 4.4B. Similar to SEM, TEM images showed that most of AuNPs were spherical in shape and the average size calculated from TEM data was 14.79 nm (n=48).

The energy dispersive spectrum in Figure 4.5 exhibits clear identification of the elemental compositions in the synthesized nanoparticles, suggesting the presence of gold (Au). Other than gold element, the spectrum also revealed the signals of carbon (C), nitrogen (N), oxygen (O) and chlorine (Cl). These elemental compositions could be arisen from X-ray emission from macromolecules like proteins/enzymes bound to the NPs or near the particles.

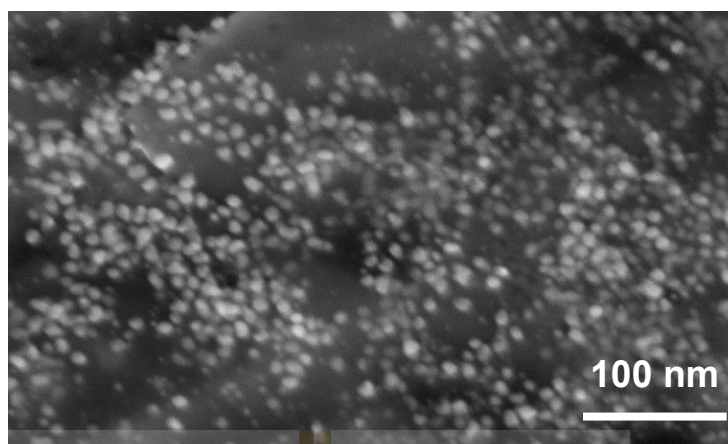


Figure 4.3 SEM image of the AuNPs (10000x).

4.4 Particle size

Figure 4.6 represents dynamic light scattering result based on intensity, volume and number weighted in colloidal solution. The average size distribution of AuNPs was found to be 61.39 nm with the zeta potential of -23 mV.

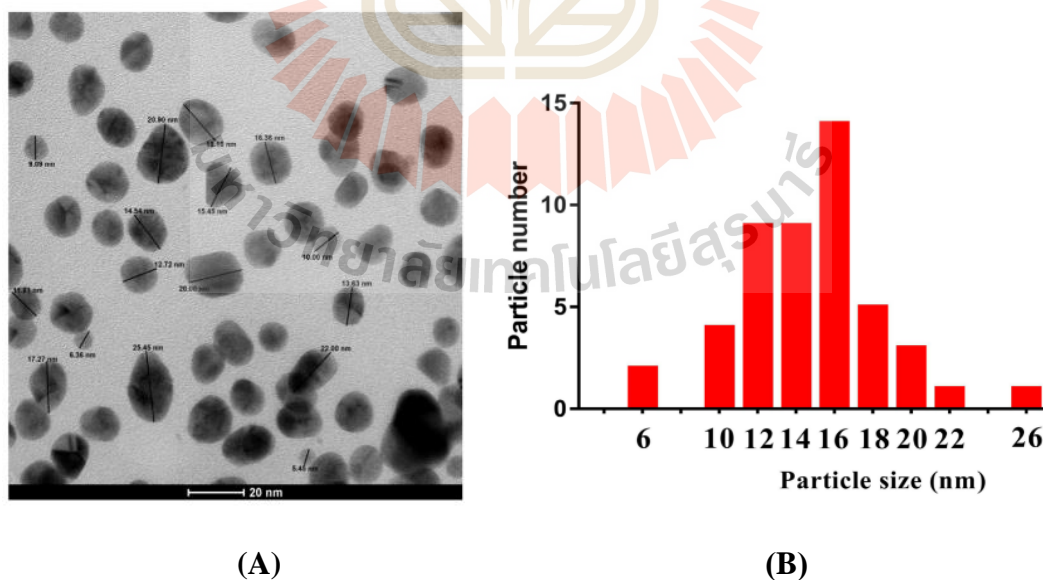


Figure 4.4 TEM image of AuNPs formed after 24 h of the bio-reduction using 1.5 ml of *C. xanthorrhiza* rhizomes extract (A). The particle size distribution histogram corresponding (B).

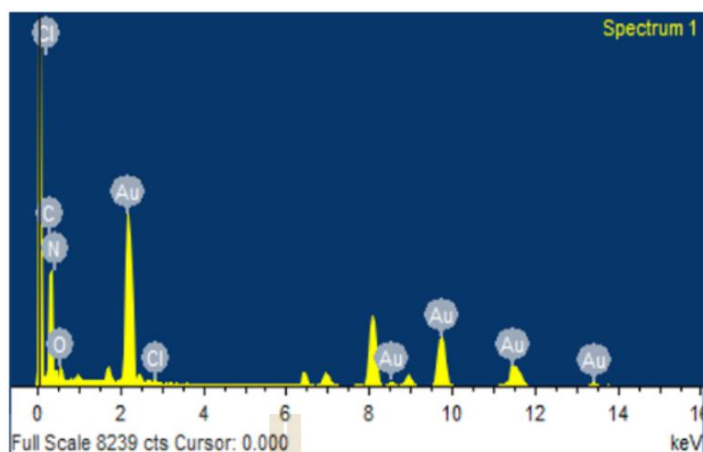
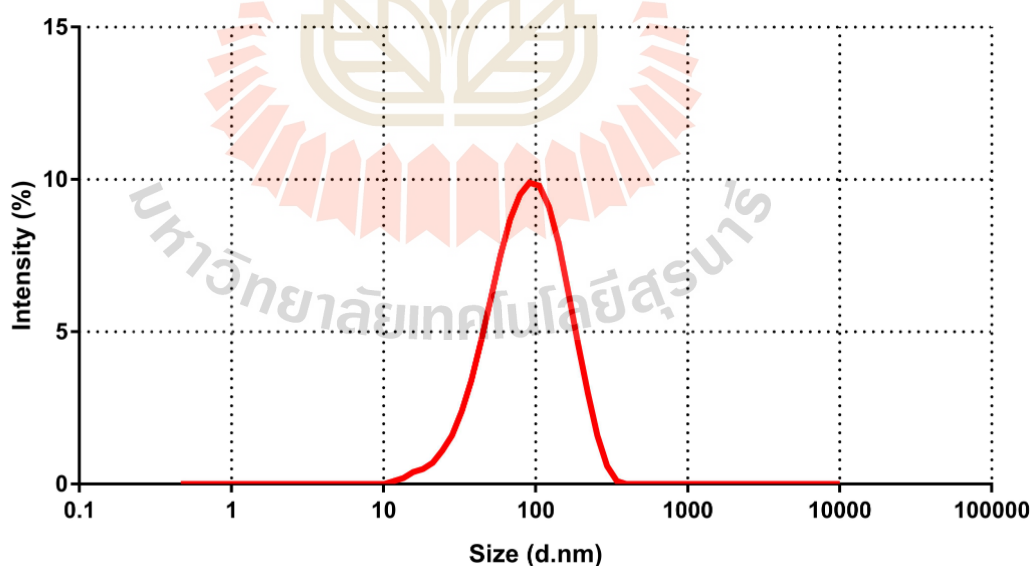


Figure 4.5 Energy dispersive spectra of AuNPs obtained from *C. xanthorrhiza* rhizomes extract. Five elements were detected in the EDX spectrum, including chloride, carbon, oxygen, nitrogen and aurum (gold), confirming the presence of aurum in the powder of synthesized AuNPs.



	Size (d.nm):	% Intensity	Width (d.nm):
Z-Average (d.nm): 61.39	Peak 1: 86.43	100.0	47.67
Pdl: 0.272	Peak 2: 0.000	0.0	0.000
Intercept: 0.925	Peak 3: 0.000	0.0	0.000

Figure 4.6 The particle size distribution of AuNPs as measured by DLS.

4.5 FTIR analysis

FTIR spectroscopy was performed to determine the possible functional group involved in the reduction and stabilization of AuNPs. The blue line in Figure 4.7 represents FTIR spectrum of *C. xanthorrhiza* rhizomes powder. Four major absorption peak shifts were observed at 3291, 2926, 1234, and 1007 to 3271, 2917, 1218, and 1029 cm^{-1} , respectively, which represents the various functional group such as O-H stretching of alcohols (3291) and phenols (2926), C-H group (1234), and C-O (1007) (Yiing Yee, Periasamy, and Abd Malek, 2014).

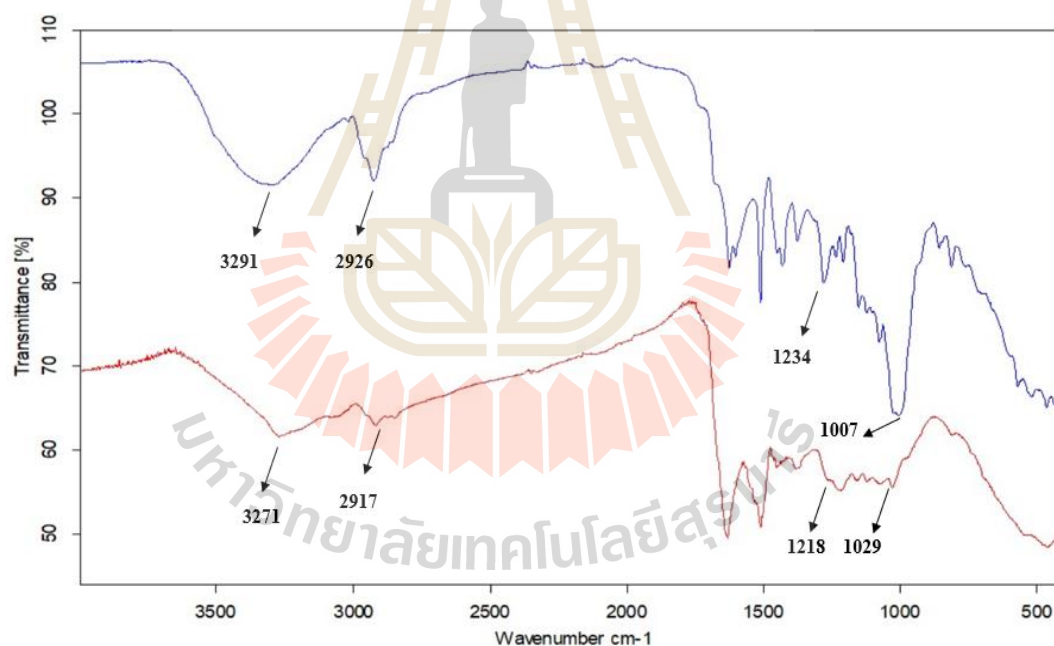
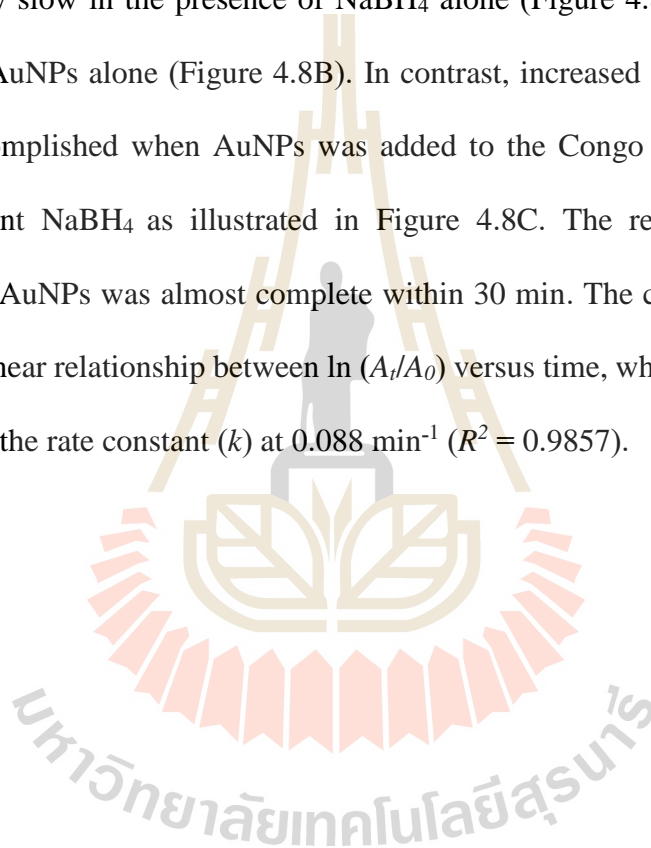


Figure 4.7 FTIR spectra of AuNPs synthesized by *C. xanthorrhiza* rhizomes extract (red) and *C. xanthorrhiza* rhizomes powder (blue).

4.6 Catalytic activity of the synthesized AuNPs

In this study, the catalytic activity of biosynthesized AuNPs was investigated for reduction of Congo red, which can be observed by a color change from red to colorless. Time-course reaction rate was monitored for 30 min by spectrophotometer. The λ_{\max} of Congo red was found at 498 nm. As shown in Figure 4.8A, degradation of the azo dye occurred very slow in the presence of NaBH_4 alone (Figure 4.8A), as well as in the presence of AuNPs alone (Figure 4.8B). In contrast, increased degradation of Congo red was accomplished when AuNPs was added to the Congo red solution with the reducing agent NaBH_4 as illustrated in Figure 4.8C. The reaction of Congo red catalyzed by AuNPs was almost complete within 30 min. The curve shown in Figure 4.7D is the linear relationship between $\ln(A_t/A_0)$ versus time, which follows first-order kinetics with the rate constant (k) at 0.088 min^{-1} ($R^2 = 0.9857$).



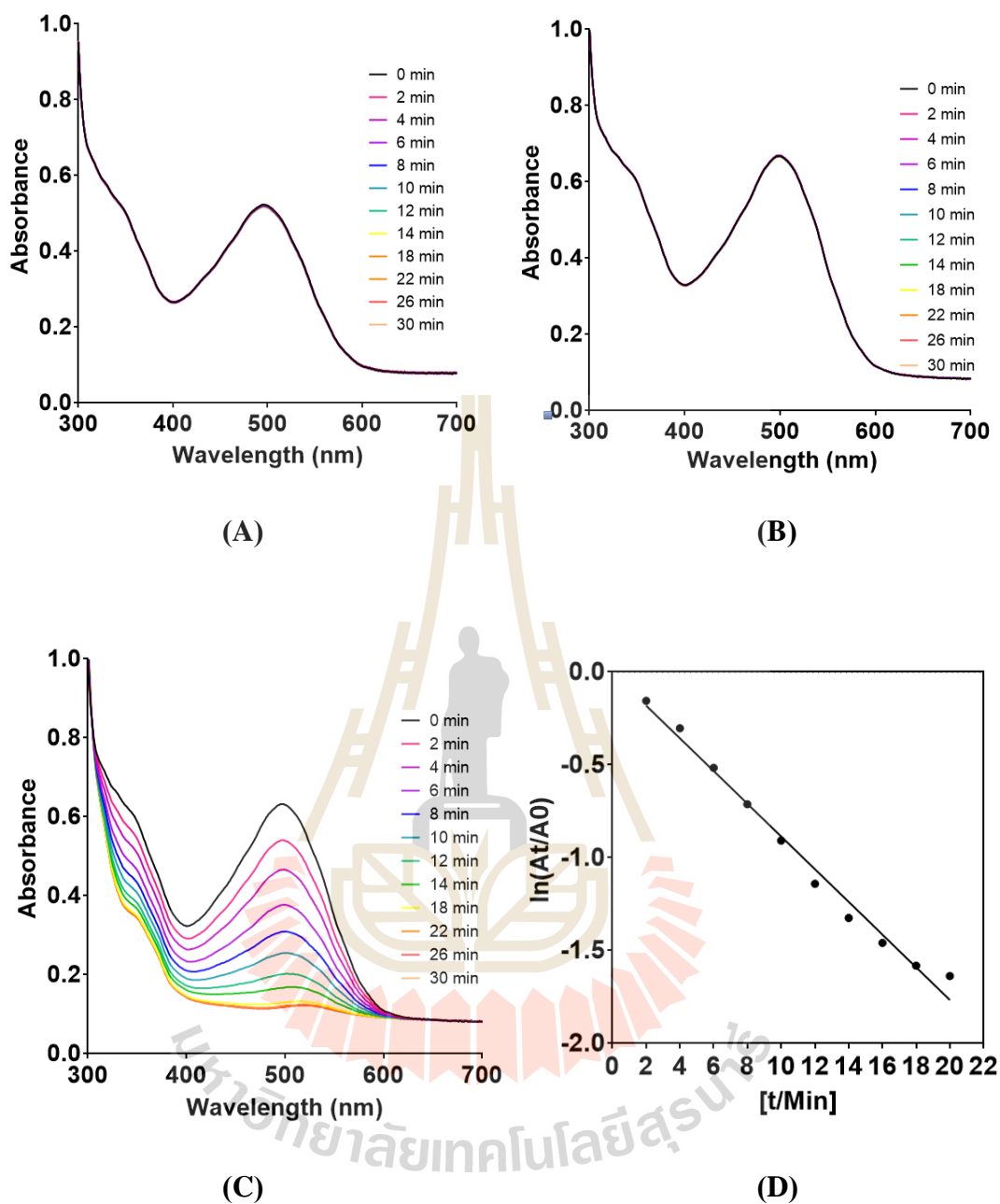


Figure 4.8 The absorbance of Congo red versus time in the presence of NaBH_4 (A), AuNPs (B) and AuNPs + NaBH_4 (C). Panel D represents the relationship between $\ln(A_t/A_0)$ versus time for the catalytic degradation of Congo red by green synthesized AuNPs.

4.7 Antibacterial activity of AuNPs

Antibacterial activities of AuNPs synthesized by using *C. xanthorrhiza* rhizomes were evaluated by a disc diffusion assay. As shown in Figure 4.9 and Table 4.1, unlike the standard antibacterial ampicillin and kanamycin against Gram-positive and Gram-negative pathogens, respectively, AuNPs or *C. xanthorrhiza* rhizomes extract caused no inhibition zones in all bacteria tested, *S. aureus*, *B. cereus*, *E. coli*, and *E. aerogenes*.

Table 4.1 Antibacterial activity of AuNPs by disc diffusion method.

No.	Strains	Zone of inhibition (mm)			
		Positive control (10 µg)	AuNPs (60 µg)	Negative control	<i>C. xanthorrhiza</i> rhizomes extract (40 µg)
1	<i>S. aureus</i>	36.67±0.88	-	-	-
2	<i>B. cereus</i>	9.67±0.88	-	-	-
3	<i>E. coli</i>	14.67±0.33	-	-	-
4	<i>E. aerogenes</i>	13.67±0.88	-	-	-

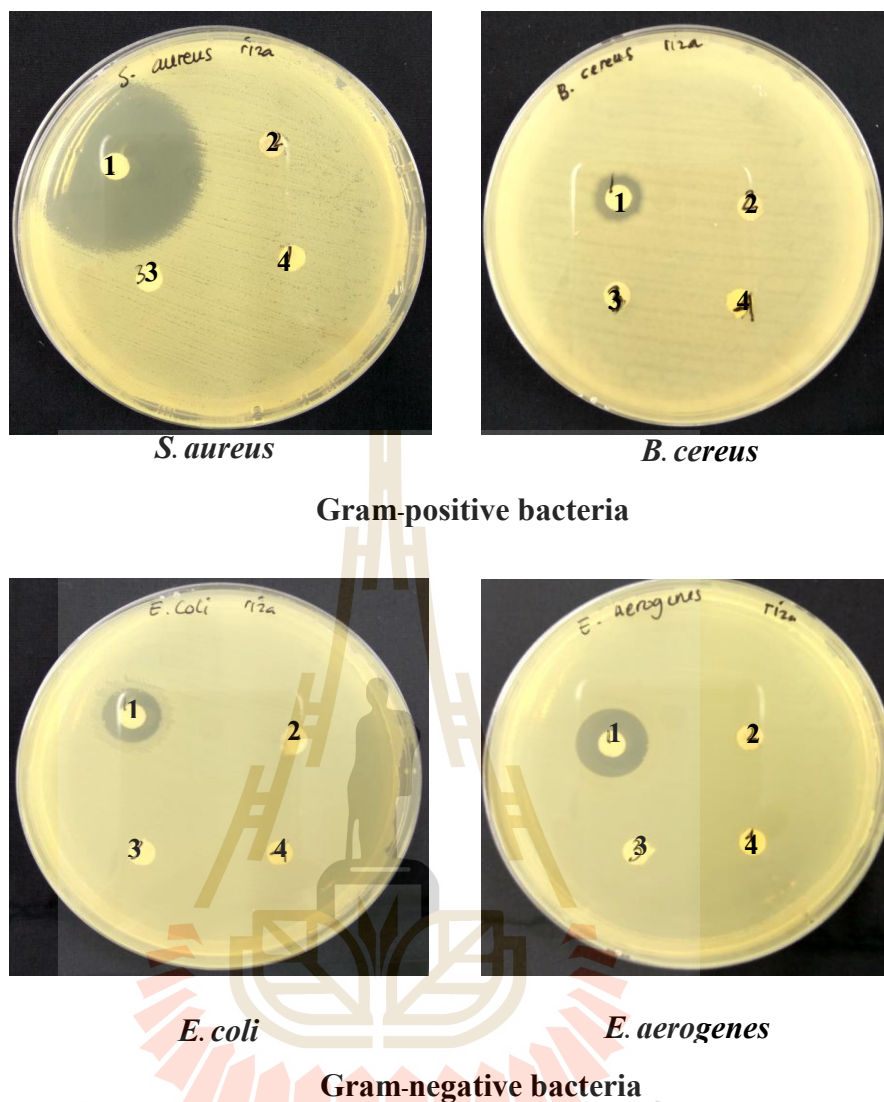


Figure 4.9 Antibacterial activity test of biosynthesized AuNPs. Unlike the standard drugs which are labelled as disc 1 (ampicillin and kanamycin for Gram-positive and Gram-negative bacteria, respectively), the synthesized AuNPs (2; 60 μg), *C. xanthorrhiza* rhizomes extract (4; 40 μg), and deionized water (3) did not show any activity against all bacteria tested.

4.8 Cytotoxicity study

Cytotoxicity study of AuNPs synthesized by using *C. xanthorrhiza* on 4T1, HepG2 and HDFa cells was examined by MTT assay (Figure 4.10A) and trypan blue (TB) exclusion method (Figure 4.10B). Different concentrations of AuNPs (0-5 $\mu\text{g/ml}$) were used to study the cytotoxicity of AuNPs. In this study, AuNPs synthesized using *C. xanthorrhiza* did not show any cytotoxicity against 4T1, HepG2 and HDFa cells (Figure 4.10A and 4.10B) at concentration of 5 $\mu\text{g/ml}$ for 24 h exposure. Moreover, it seems to increase proliferation of HDFa cells when examined by MTT assay at high concentrations. In contrast, the results from TB method did not show any stimulatory effect on proliferation compared with control. This discrepancy raised a doubt in an interference of MTT assay by the absorption of AuNPs. Figure 4.11 gives direct evidence that AuNPs tightly attached on the surface of HDFa cells. UV-vis spectroscopy measurement of AuNPs was also conducted (Figure 4.12) and the results reveals that the absorbance at 495 nm increased with the increasing concentrations. Thus, the cytotoxicity of the synthesized AuNPs in this study will further rely only on the TB exclusion method.

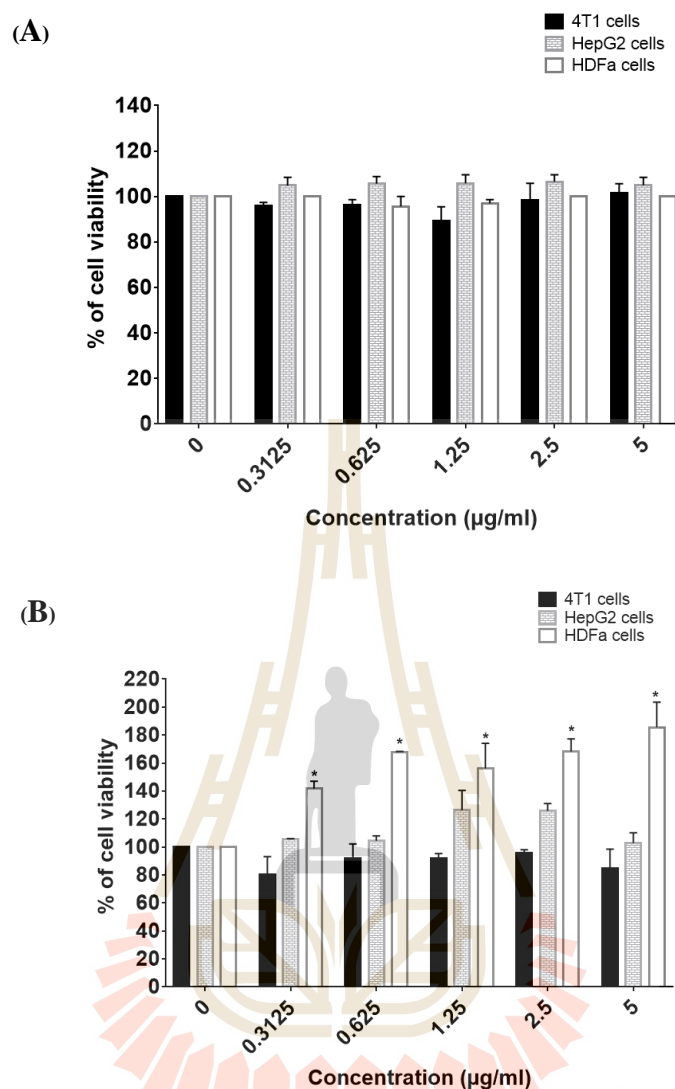


Figure 4.10 Cytotoxicity effects of the biosynthesized AuNPs. Unlike the results from MTT assay (Panel A), that from Trypan blue exclusion method revealed that AuNPs at concentrations of 0.3125- 5 µg/ml did not show any effect on cell viability of 4T1, HepG2 and HDFa cells for 24 h. Noted that, the calculated % of cell viability from MTT assay appeared to be interfered by the absorbance of the nanoparticles at 570 nm as mentioned in the text. The values are expressed as mean \pm SEM, n=3.

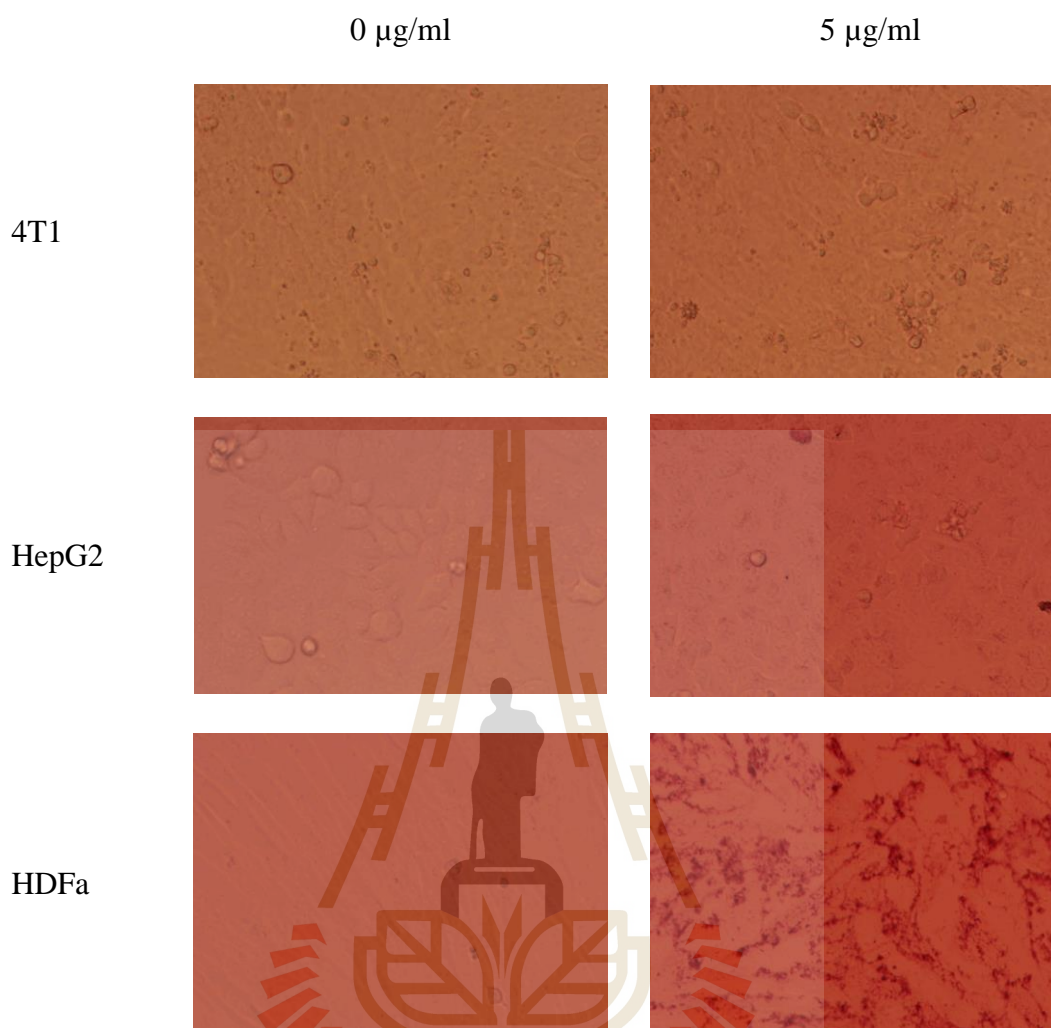


Figure 4.11 Microscopic images of 4T1, HepG2 and HDFa cells after the exposure of synthesized AuNPs (5 $\mu\text{g/ml}$) for 24 h. It was clearly seen that the nanoparticles attached to HDFa cells much more than to 4T1 and HepG2 cells.

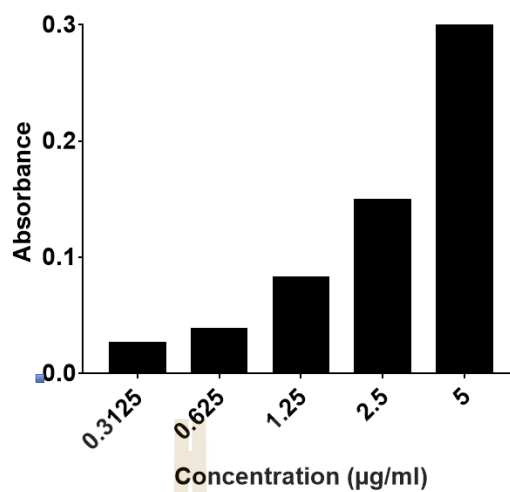


Figure 4.12 UV-visible absorption of the concentrations of AuNPs used in MTT method at 570 nm.

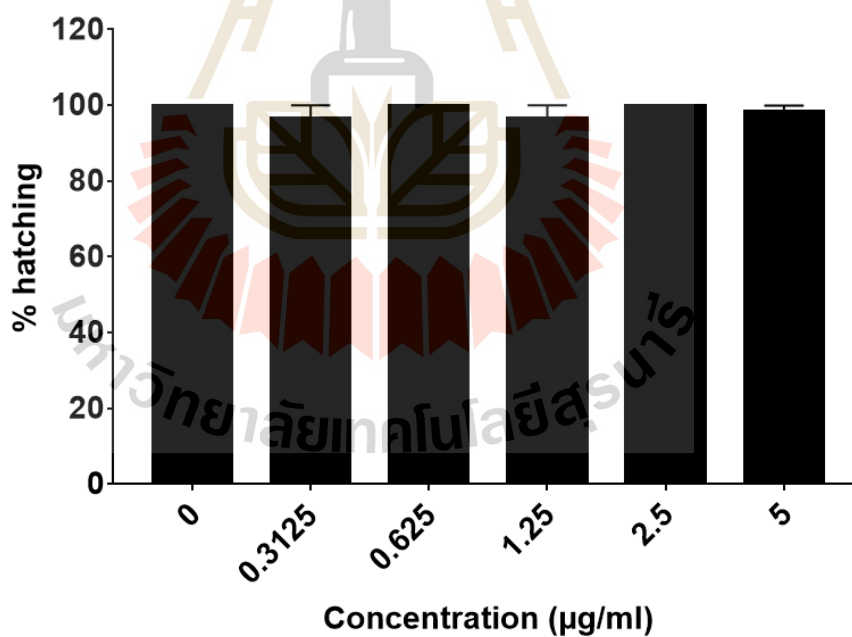


Figure 4.13 The effect of the synthesized AuNPs on hatching rate of zebrafish embryos. The embryos were exposed with different concentrations of AuNPs for 96 h. The result showed that the AuNPs had no effect on the hatching of zebrafish embryos. The values are expressed as mean \pm SEM, n=3.

4.9 *In vivo* study on zebrafish embryos

In this work, zebrafish embryo model was used to determine whether the biosynthesized AuNPs using *C. xanthorrhiza* had any toxicity effect on development *in vivo*. After four days observation, there is no significant difference in the hatching rate between control (100%) and AuNPs exposed groups (98.33%), as presented in Figure 4.13. The results in Figure 4.14 revealed that AuNPs at a concentration up to 5 $\mu\text{g/ml}$, which was 10 times higher than that in the catalytic study, caused no toxicity or malformation compared to the control group.



Figure 4.14 Development of zebrafish embryos during 4 days of AuNPs exposure with 20x magnification.

CHAPTER V

DISCUSSION

Method for AuNPs synthesis was first discovered by Faraday in 1857 which used sodium citrate as reducing agent as well as a stabilizing agent. However, this method might lead to high cost and toxic byproducts, harmful to the environment and not compatible in biomedical applications. Therefore, biosynthesis is an alternative for replacement of toxic chemical methods due to its low cost, ecofriendly and biocompatibility (Kumar et al., 2016). Biosynthesis can be employed by using either plant tissues (such as leaf, stem, fruit, bark, root, peel, flower, etc.) or microorganisms (such as yeast, bacteria, fungi, etc.) (Ahmed et al., 2016). Phytosynthesis using plant extracts has some advantage because it can easily be scaled up for large scale synthesis without requiring any cell culture compared to the method using microorganisms. However, this method has many key factors such as concentration of extract, metal salt concentration, reaction time, pH, and temperature, which can influence the quality, size, and morphology of the synthesized nanoparticles. For example, larger particles tend to be produced at a lower acidic pH values compared to high pH values (Shah et al., 2015). In this study, optimization of AuNPs by phytosynthesis method using *C. xanthorrhiza* extract (crude extract) was performed.

The green synthesis of AuNPs was successfully conducted using HAuCl_4 and crude extract as the precursor and reducing agent, respectively. Strong alkali solution is needed to extract the active ingredients, which act as reducing agents. The extract

must be freshly prepared and immediately used due to its fast degradation (Cheuh et al., 2013). The formation of AuNPs can be visually observed. The colour of the solution changed from yellow-brown (extract alone) to light violet or ruby red, within 30 min. This can also be measured by UV-Vis spectroscopy which is one of the crucial tools to confirm the formation and stability of metal nanoparticles in aqueous solution. Figure 4.1A shows the effect of various concentrations of the extract was used with 1 mM HAuCl₄. It is widely known that the higher concentration of the reducing agent, the smaller size of gold nanoparticles will be produced. In the present study, as the amount of the extract was increased, the λ_{\max} shifted to a lower wavelength from 557 to 538 nm. However, the data in Figure 4.1A suggested that the optimal concentration of *C. xanthorrhiza* rhizomes extract with 0.1 mM HAuCl₄ (final concentration) was 1.5 ml as the peak at λ_{\max} was decreased when the higher concentration was added. When studied this optimal concentration and time was chosen for all of further experiments.

Crystalline nanostructure of the AuNPs biologically synthesized in the present study was further confirmed using XRD analysis by comparing diffraction data against a database. The characteristic diffraction peaks of AuNP sample were located at 38.19°, 44.39°, 64.58°, 77.57° and 81.73° (Figure 4.2) which correspond to (111), (200), (220), (311), and (222) reflections of face centered cubic (FCC) structure of metallic gold, respectively. These results clearly revealed that AuNPs were formed. The (111) plane is higher compared with others which is the predominant orientation with FCC symmetry and high degree of crystallinity (Kumar et al., 2016). The average size of AuNPs was found to be approximately 10 nm. Its size was calculated using the Debye Scherrer formula (below) which is estimation from the line broadening spectrum of the reflection.

Debye Scherrer formula: $D = 0.94k/\beta \cos \Theta$,

where D is the average crystallite size, k is the X-ray wavelength, β is the full width at half maximum and Θ is the diffraction angle (Gopinath, Priyadarshini, Meera Priyadharsshini, Pandian, and Velusamy, 2013).

The morphology and size of AuNPs is shown in Figures 4.3, 4.4A, and 4.4B. The TEM and SEM images exhibited almost spherical shape of particles within the range of 5.45-25.45 nm (n=48), with a size of 14.79 ± 3.65 nm. The size distribution of the AuNPs was determined using dynamic light scattering (DLS) as illustrated in Figure 4.6. The average size of the AuNPs obtained in this study was 61.39 nm which was larger when compare to the calculated size from XRD and TEM methods. Due to the size of particles that measured by DLS includes the hydrodynamic size and the bio-organic compounds enveloping the core of the AuNPs (Sujitha and Kannan, 2013).

Chemical analysis of the produced AuNPs was achieved by means of EDXRF, which confirmed both the presence of Au and the organic composition which serve as capping and stabilizing agent that is evidenced by the presence of C, O, and N peaks is presented in the Figure 4.5. To give more evidence for the reduction of chloroauric acid to elemental gold, chemical analysis of the product was subjected to FTIR analysis. The data in Figure 4.7 confirmed the possible interaction between AuNPs and bioactive molecules in the extract. The FTIR spectra of crude extract and AuNPs showed the absorption peaks at 3291, 2916, 1234, and 1007; and 3271, 2917, 1218, and 1029 cm^{-1} , respectively. The intense bands at 3291 and 3271 cm^{-1} are characteristic of O-H stretching of primary alcohol, while those at 2926 and 2917 cm^{-1} are of phenol. The peaks at 1234 and 1218 cm^{-1} correspond to C-H stretching vibration of hydrocarbon bond. The absorption peaks at 1007 and 1029 can be attributed to the stretching

vibration of C-O. Moreover, it was suggested that when hydroxyl groups were reduced and converted to aldehyde or carboxylic groups, the peak around 3000 nm^{-1} became broader and the peak at 1007 nm^{-1} disappeared (Yiing Yee, Periasamy, and Abd Malek, 2014).

Several bioorganic compounds from plant such as flavonoids, terpenoids, proteins, reducing sugars and alkaloids can act as either reducing or capping agents during the formation of nanoparticles. Curcumin is a diarylheptanoid (terpenoids) which is also found in *C. xanthorrhiza* rhizomes. It contributes to the scent, flavor and color and is suggested to be responsible for reducing the Au^{3+} to Au^0 (Gan and Li, 2012). Similarly with the previous study reported that terpenoid from *Szygium aromaticum* can act as reducing agent during the formation of AuNPs (Singh, Talat, Singh, and Srivastava, 2010). However, other active compounds in the extract may also contribute to the phyto-reduction of the precursor HAuCl_4 . In addition to their reducing property, these bioorganic compounds can contribute as a stabilizer. In this study, the stability of AuNPs suspension is up to one month as no precipitation was seen during the storage at room temperature.

The catalytic activity of the obtained AuNPs was further examined for degradation of azo dye. The reduction of Congo red can be observed by a color change from red to colorless within 30 min (Figure 4.8A). During the reduction reaction, increasing degradation of Congo red was observed when both AuNPs and NaBH_4 were added into the dye solution shown as the band at 498 nm gradually disappeared (Figure 4.8C). As seen in the absence of catalyst, there was a very slow decrease of absorbance of Congo red solution, indicating that this dye is not reduced effectively by NaBH_4 (Figure 4.8A) or AuNPs (Figure 4.8B) alone. From the plot of $\ln(A_t/A_0)$ versus time, the rate constant

(*k*) found to be 0.088 min^{-1} ($R^2 = 0.9857$). The reduction kinetics can be considered as a first order rate law with regard to Congo red alone.

The biogenic AuNPs showed catalytic reduction of Congo red. This result is accordance with the results from previous studies (Guo et al., 2015); (Nadaf and Kanase, 2016). Similar to the present study, the degradation of Congo red was complete within 30 and 20 min in the presence of AuNPs in the size of 16.4 and 32 nm, respectively. The specific reaction mechanism as catalyst of AuNPs is not completely understood. One possible mechanism may be due to the intermediate redox potential of AuNPs between the electron donor BH_4^- and the acceptor Congo red can assist in the electron transfer and act as an electron relay system, resulting that azo double $-\text{N}=\text{N}-$ bonds were reduced as the $-\text{NH}-\text{HN}-$ bonds, and the dye was disappeared (Guo et al., 2015). It has been reported that there are three factors affecting adsorption of dyes onto AuNPs, namely: particle size, molecular weight of dyes, and the effect of pH (Thompson, 2007). In this study, the size of AuNP with the average size about 16 nm and pH of the catalytic solution at about 9.8 produced first order kinetic reaction.

Antibacterial activities of AuNPs synthesized by using *C. xanthorrhiza* rhizomes were tested against Gram-positive and Gram-negative bacteria by a disc diffusion assay. The result showed that the synthesized AuNPs did not produce antibacterial activity on any bacteria tested with the doses up to $60 \mu\text{g}/\text{disc}$ (Figure 4.9). Many reports demonstrated that AuNPs exhibited antibacterial effects against several pathogen bacteria, such as *S. aureus*, *B. subtilis*, *B. cereus*, *E. coli*, *P. aeruginosa*, *Proteus vulgaris*. However, some studies showed no antibacterial activity of AuNPs. This discrepancy may be due to the different physicochemical properties of nanoparticles in each study that plays an important role in tolerance or susceptibility of bacteria (Dorosti

and Jamshidi, 2016). The structure of the cell wall also plays an important role in this context. Moreover, the rate of bacterial growth appears to be crucial, where fast growing bacteria are more susceptible to nanoparticles compared to slow growing bacteria, as well as the capability of bacteria to produce biofilms. Biofilms are a complex microbial community that is formed by adhesion to a solid surface and by secretion of a matrix (protein, DNA, and extra polysaccharide), which cover the bacterial cell community (Hajipour et al., 2012). There are at least two modes of action that have been proposed: the first is to change membrane potential and inhibit ATP synthase activities, resulting in a decrease of ATP level and subsequently a general decline in metabolism. The second is to inhibit the subunit of ribosome for tRNA binding, indicating a collapse of biological process (Cui et al., 2012). The mechanism underlying antibacterial action of AuNPs is still a topic of interest to the scientific community.

Regarding the divergent effects of AuNPs, the surface of nanoparticles has also been proposed to play a role for their antibacterial activities. The molecules that act as capping agents which are surrounding the nanoparticles probably affect, at least partly, to their activities. In this study, unlike the positive controls, *C. xanthorrhiza* rhizomes extract did not inhibit Gram-positive or Gram-negative. In this green synthesis which using this plant extract as reducing agents, phytochemicals such as flavonoids, terpenoids or tannin, which showed no effect on bacteria may prevent the direct exposure and penetration of gold nanoparticle to bacteria.

For biocompatibility, cytotoxicity activities of this biosynthesized AuNPs were tested against three types of mammalian cells (4T1, HepG2, and HDFa cells). Breast cancer 4T1 cells are easily transplanted into the mammary gland so that the primary

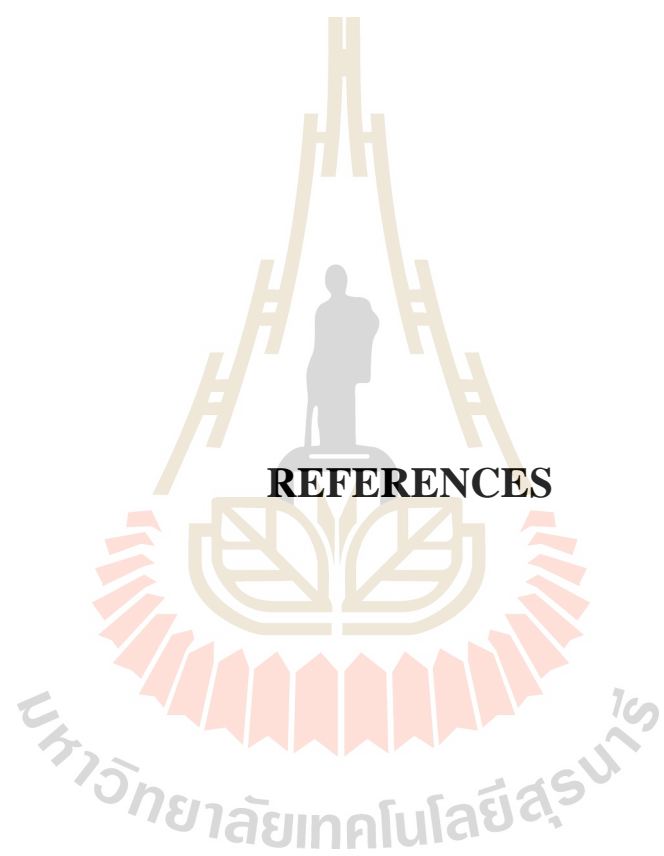
tumor grows in the anatomically correct site. On the other hand, it can spontaneously metastasize from the primary tumor in the mammary gland to multiple distant sites including lymph nodes, blood, liver, lung, brain, and bone (Pulaski and Ostrand-Rosenberg, 2001). The primary tumor of these cells metastasizes as early as 2 weeks (after inoculation) to organ such as lungs, liver, bone, and brain (Baliga, Meleth, and Katiyar, 2005). In contrast, HepG2 is derived from the liver tissue of a 15-year-old Caucasian male who had a well-differentiated hepatocellular carcinoma. These cells contain 55 chromosome pairs, and secrete many plasma proteins, such as transferrin, fibrinogen, plasminogen and albumin (Bouma, Rogier, Verthier, Labarre, and Feldmann, 1989). Different from HepG2 and 4T1 cells, HDFa is fibroblast cell type from human skin which can be used as a suitable healthy control for molecular cellular studies (Adinolfi, Pellegrino, and Baldini, 2015).

Cytotoxicity study of AuNPs synthesized by using *C. xanthorrhiza* was examined by MTT assay (Figure 4.10A) and trypan blue (TB) exclusion method (Figure 4.10B). The results revealed that the AuNPs produced no toxicity against any of the cell types tested. Interestingly, it increased proliferation of HDFa cells in MTT assay. It might be the characteristic of HDFa cell surface can be easily stucked with AuNPs compared 4T1 and HepG2 cells, as showed in Figure 4.11. There was no toxicity when three of the cells exposed to AuNPs for 24 h. As described in the section 2.5, toxicity reports of AuNPs are controversial. It has been suggested that the cytotoxicity effect of AuNPs depends on the dose or size of AuNPs. Moreover, it was claimed that the surface electric charge can be a key factor in a toxicity study of AuNPs. The AuNPs tested in the latter study contained positively charged functional groups which was believed to increase their ability to interact with the organisms (García-Camero et al., 2013). In this study,

the functional groups on the nanoparticles have not yet identified and need more investigated.

Biocompatibility of the biosynthesized AuNPs was further evaluated in zebrafish model. Zebrafish embryos treated with AuNPs did not show any toxicity or malformation even the concentration was increased to 5 $\mu\text{g/ml}$ (Figure 4.13 and 4.14). AuNPs seem to be much less toxicity than AgNPs. AgNPs synthesized by *Spinacia oleracea* at 3 $\mu\text{g/ml}$ caused 100% mortality and yolk sac edema. In contrast, AuNPs at 300 mg/ml which is 60,000 times higher than the concentration used in this study started to exhibit the same effects as AgNPs did (Ramachandran et al., 2017). Differently, AuNPs with a core diameter of 1.5 nm and functionalized with either trimethylammoniummethanethiol (TMAT-AuNPs) or 2-mercaptoethanesulfonic acid (MES-AuNPs) by chemically synthesis method, exhibited hypo-locomotor activity at 50 $\mu\text{g/ml}$ and 10 $\mu\text{g/ml}$, respectively (Truong et al., 2012). Therefore, this study has added more direct evidence that the green synthesized AuNPs could be considered as high biocompatible when testing with zebrafish model.

In conclusion, non-expensive and simple method was successfully used to synthesize AuNPs nanoparticles by *C. xanthorrhiza* rhizomes extract at room temperature. The obtained AuNPs had particle size around 16 nm and mostly in spherical shape. These nanoparticles have potential catalytic activity in discoloration of Congo red by NaBH_4 . The overall results confirm that the extract of *C. xanthorrhiza* rhizomes can be used as a bio-reduction agent to form biocompatible AuNPs as shown in zebrafish embryos and cytotoxicity test in 4T1, HepG2, and HDFa cells. The catalytic activity of the obtained AuNPs will be useful for industrial applications as well as nanoscience and nanotechnology.



REFERENCES

REFERENCES

- Abdel-Raouf, N., Al-Enazi, N. M., and Ibraheem, I. B. M. (2017). Green biosynthesis of gold nanoparticles using *Galaxaura elongata* and characterization of their antibacterial activity. **Arabian Journal of Chemistry**. 10: S3029-S3039.
- Adinolfi, B., Pellegrino, M., and Baldini, F. (2015). Human dermal fibroblasts HDFa can be used as an appropriate healthy control for PMMA nanoparticles-survivin molecular beacon cellular uptake studies. **Biomedicine and Pharmacotherapy**. 69: 228-232.
- Aguar Fernandez, M. P., and Hullmann, A. (2007). A boost for safer nanotechnology. **Nano Today**. 2(1): 56.
- Ahmad, A., Wei, Y., Ullah, S., Shah, S. I., Nasir, F., Shah, A., Iqbal, Z., Tahir, K., Khan, U.A., and Yuan, Q. (2017). Synthesis of phytochemicals-stabilized gold nanoparticles and their biological activities against bacteria and Leishmania. **Microb Pathog**. 110: 304-312.
- Ahmed, S., Annu, Ikram, S., and Yudha S, S. (2016). Biosynthesis of gold nanoparticles: A green approach. **Journal of Photochemistry and Photobiology B: Biology**. 161: 141-153.
- Alkilany, A. M., and Murphy, C. J. (2010). Toxicity and cellular uptake of gold nanoparticles: what we have learned so far? **Journal of Nanoparticle Research**. 12(7): 2313-2333.

- Araujo, C. C., and Leon, L. L. (2001). Biological activities of *Curcuma longa* L. **Memórias Do Instituto Oswaldo Cruz**. 96(5): 723-728.
- Ashokkumar, T., Prabhu, D., Geetha, R., Govindaraju, K., Manikandan, R., Arulvasu, C., and Singaravelu, G. (2014). Apoptosis in liver cancer (HepG2) cells induced by functionalized gold nanoparticles. **Colloids Surf B Biointerfaces**. 123: 549-556.
- Badwaik, V. D., Vangala, L. M., Pender, D. S., Willis, C. B., Aguilar, Z. P., Gonzalez, M. S., Paripelly, R., and Dakshinamurthy, R. (2012). Size-dependent antimicrobial properties of sugar-encapsulated gold nanoparticles synthesized by a green method. **Nanoscale Research Letters**. 7(1): 623.
- Baliga, M. S., Meleth, S., and Katiyar, S. K. (2005). Growth inhibitory and antimetastatic effect of green tea polyphenols on metastasis-specific mouse mammary carcinoma 4t1 cells *in vitro* and *in vivo* systems. **Clinical Cancer Research**. 11(5): 1918.
- Bhawana, Basniwal, R. K., Buttar, H. S., Jain, V. K., and Jain, N. (2011). Curcumin nanoparticles: preparation, characterization, and antimicrobial study. **Journal of Agricultural and Food Chemistry**. 59(5): 2056-2061.
- Bindhu, M. R., and Umadevi, M. (2014). Antibacterial activities of green synthesized gold nanoparticles. **Materials Letters**. 120: 122-125.
- Bouma, M.-E., Rogier, E., Verthier, N., Labarre, C., and Feldmann, G. (1989). Further cellular investigation of the human hepatoblastoma-derived cell line HepG2: Morphology and immunocytochemical studies of hepatic-secreted proteins. **In Vitro Cellular and Developmental Biology**. 25(3): 267-275.

- Ch, L., Goel, N., Datta, K. K. R., Addlagatta, A., Ummanni, R., and V. Subba Reddy, B. (2013). Green Synthesis of Curcumin Capped Gold Nanoparticles and Evaluation of Their Cytotoxicity **Nanoscience and Nanotechnology Letters**. 5(12): 1258-1265.
- Chakraborty, C., Sharma, A. R., Sharma, G., and Lee, S.-S. (2016). Zebrafish: a complete animal model to enumerate the nanoparticle toxicity. **Journal of Nanobiotechnology**. 14(1): 65.
- Chuang, S. M., Lee, Y. H., Liang, R. Y., Roam, G. D., Zeng, Z. M., Tu, H. F., Wang, S. K., and Chueh, P. J. (2013). Extensive evaluations of the cytotoxic effects of gold nanoparticles. **Biochimica et Biophysica Acta**. 1830(10): 4960-4973.
- Chudapongse, N., Kamkhunthod, M., and Poompachee, K. (2010). Effects of *Phyllanthus urinaria* extract on HepG2 cell viability and oxidative phosphorylation by isolated rat liver mitochondria. **Journal Ethnopharmacology**. 130(2): 315-319.
- Chueh, P. J., Liang, R. Y., Lee, Y. H., Zeng, Z. M., and Chuang, S. M. (2014). Differential cytotoxic effects of gold nanoparticles in different mammalian cell lines. **Journal of Hazard Materials**. 264: 303-312.
- Connor, E. E., Mwamuka, J., Gole, A., Murphy, C. J., and Wyatt, M. D. (2005). Gold nanoparticles are taken up by human cells but do not cause acute cytotoxicity. **Small**. 1(3): 325-327.
- Coradeghini, R., Gioria, S., Garcia, C. P., Nativo, P., Franchini, F., Gilliland, D., Ponti, J., and Rossi, F. (2013). Size-dependent toxicity and cell interaction mechanisms of gold nanoparticles on mouse fibroblasts. **Toxicology Letters**. 217(3): 205-216.

- Cui, Y., Zhao, Y., Tian, Y., Zhang, W., Lu, X., and Jiang, X. (2012). The molecular mechanism of action of bactericidal gold nanoparticles on *Escherichia coli*. **Biomaterials**. 33(7): 2327-2333.
- Das, S., Pandey, A., Pal, S., Kolya, H., and Tripathy, T. (2015). Green synthesis, characterization and antibacterial activity of gold nanoparticles using hydroxyethyl starch-g-poly (methylacrylate-co-sodium acrylate): a novel biodegradable graft copolymer. **Journal of Molecular Liquids**. 212: 259-265.
- Dorosti, N., and Jamshidi, F. (2016). Plant-mediated gold nanoparticles by *Dracocephalum kotschy* as anticholinesterase agent: synthesis, characterization, and evaluation of anticancer and antibacterial activity. **Journal of Applied Biomedicine**. 14(3): 235-245.
- Dykman, L. A., and Khlebtsov, N. G. (2011). Gold nanoparticles in biology and medicine: recent advances and prospects. **Acta Naturae**. 3(2): 34-55.
- Faramarzi, M. A., and Forootanfar, H. (2011). Biosynthesis and characterization of gold nanoparticles produced by laccase from *Paraconiothyrium variabile*. **Colloids and Surfaces B: Biointerfaces**. 87(1): 23-27.
- Foo, Y. Y., Periasamy, V., Kiew, L. V., Kumar, G. G., and Malek, S. N. A. (2017). *Curcuma mangga*-mediated synthesis of gold nanoparticles: characterization, stability, cytotoxicity, and blood compatibility. **Nanomaterials**. 7(6): 123.
- Fraga, S., Faria, H., Soares, M. E., Duarte, J. A., Soares, L., Pereira, E., Costa- Pereira, C., Teixeira, J. P., de Lourdes, B. M., and Carmo, H. (2013). Influence of the surface coating on the cytotoxicity, genotoxicity and uptake of gold nanoparticles in human HepG2 cells. **Journal of Applied Toxicology**. 33(10): 1111-1119.

- Fratoddi, I., Venditti, I., Cametti, C., and Russo, M. V. (2015). How toxic are gold nanoparticles? The state-of-the-art. **Nano Research**. 8(6): 1771-1799.
- Gan, P. P., and Li, S. F. Y. (2012). Potential of plant as a biological factory to synthesize gold and silver nanoparticles and their applications. **Reviews in Environmental Science and Bio/Technology**. 11(2): 169-206.
- Ganeshkumar, M., Sastry, T. P., Sathish Kumar, M., Dinesh, M. G., Kannappan, S., and Suguna, L. (2012). Sun light mediated synthesis of gold nanoparticles as carrier for 6-mercaptopurine: Preparation, characterization and toxicity studies in zebrafish embryo model. **Materials Research Bulletin**. 47(9): 2113-2119.
- García-Camero, J. P., Núñez García, M., López, G. D., Herranz, A. L., Cuevas, L., Pérez-Pastrana, E., Cuadal J. S., Castelltort, M. R., and Calvo, A. C. (2013). Converging hazard assessment of gold nanoparticles to aquatic organisms. **Chemosphere**. 93(6): 1194-1200.
- Geethalakshmi, R., and Sarada, D. V. L. (2013). Characterization and antimicrobial activity of gold and silver nanoparticles synthesized using saponin isolated from *Trianthema decandra* L. **Industrial Crops and Products**. 51: 107-115.
- Ghosh, P., Han, G., De, M., Kim, C. K., and Rotello, V. M. (2008). Gold nanoparticles in delivery applications. **Advanced Drug Delivery Reviews**. 60(11): 1307-1315.
- Gopinath, K., Kumaraguru, S., Bhagyaraj, K., Mohan, S., Venkatesh, K. S., Esakkirajan, M., Kaleeswaran, P., Alharbi, N. S., and Arumugam, A. (2016). Green synthesis of silver, gold and silver/gold bimetallic nanoparticles using the *Gloriosa superba* leaf extract and their antibacterial and antibiofilm activities. **Microbial Pathogenesis**. 101: 1-11.

- Gopinath, V., Priyadarshini, S., Meera Priyadharsshini, N., Pandian, K., and Velusamy, P. (2013). Biogenic synthesis of antibacterial silver chloride nanoparticles using leaf extracts of *Cissus quadrangularis* Linn. **Materials Letters**. 91: 224-227.
- Guo, M., Li, W., Yang, F., and Liu, H. (2015). Controllable biosynthesis of gold nanoparticles from a *Eucommia ulmoides* bark aqueous extract. **Spectrochimica Acta Part A: Molecular and Biomolecular Spectroscopy**. 142: 73-79.
- Hajipour, M. J., Fromm, K. M., Ashkarran, A. A., Jimenez de Aberasturi, D., de Larramendi, I. R., Rojo, T., Serpooshan, V., Parak, W. J., and Mahmoudi, M. (2012). Antibacterial properties of nanoparticles. **Trends Biotechnology**. 30(10): 499-511.
- Hall, S. R., Shenton, W., Engelhardt, H., and Mann, S. (2001). Site-specific organization of gold nanoparticles by biomolecular templating. **Chemphyschem**. 2(3): 184-186.
- Huang, W. C., Tsai, P. J., and Chen, Y. C. (2007). Functional gold nanoparticles as photothermal agents for selective-killing of pathogenic bacteria. **Nanomedicine (Lond)**. 2(6): 777-787.
- Humeera, N., Kamili, A. N., Bandh, S. A., Amin, S. U., Lone, B. A., and Gousia, N. (2013). Antimicrobial and antioxidant activities of alcoholic extracts of *Rumex dentatus* L. **Microbial Pathogenesis**. 57: 17-20.
- Hvolbæk, B., Janssens, T. V. W., Clausen, B. S., Falsig, H., Christensen, C. H., and Nørskov, J. K. (2007). Catalytic activity of Au nanoparticles. **Nano Today**. 2(4): 14-18.

- Joseph, S., and Mathew, B. (2015). Microwave-assisted green synthesis of silver nanoparticles and the study on catalytic activity in the degradation of dyes. **Journal of Molecular Liquids**. 204: 184-191.
- Kavita, K., Singh, V. K., and Jha, B. (2014). 24-Branched Delta5 sterols from *Laurencia papillosa* red seaweed with antibacterial activity against human pathogenic bacteria. **Microbiological Research**. 169(4): 301-306.
- Khamhaengpol, A., and Siri, S. (2016). Fluorescent light mediated a green synthesis of silver nanoparticles using the protein extract of weaver ant larvae. **Journal of Photochemistry and Photobiology B**. 163: 337-344.
- Khlebtsov, N., and Dykman, L. (2011). Biodistribution and toxicity of engineered gold nanoparticles: a review of in vitro and in vivo studies. **Chemical Society Reviews**. 40(3): 1647-1671.
- Kim, D. Y., Kim, M., Shinde, S., Sung, J. S., and Ghodake, G. (2017). Cytotoxicity and antibacterial assessment of gallic acid capped gold nanoparticles. **Colloids Surf B Biointerfaces**. 149: 162-167.
- Klaus-Joerger, T., Joerger, R., Olsson, E., and Granqvist, C. (2001). Bacteria as workers in the living factory: metal-accumulating bacteria and their potential for materials science. **Trends in Biotechnology**. 19(1): 15-20.
- Kumar, B., Smita, K., Cumbal, L., Camacho, J., Hernández-Gallegos, E., de Guadalupe Chávez-López, M., Grijalva, M., and Andrade, K. (2016). One pot phytosynthesis of gold nanoparticles using *Genipa americana* fruit extract and its biological applications. **Materials Science and Engineering: C**. 62: 725-731.

- Lasagna-Reeves, C., Gonzalez-Romero, D., Barria, M. A., Olmedo, I., Clos, A., Sadagopa Ramanujam, V. M., Urayama, A., Vergara, L., Kogan, M. J., and Soto, C. (2010). Bioaccumulation and toxicity of gold nanoparticles after repeated administration in mice. **Biochemical and Biophysical Research Communications**. 393(4): 649-655.
- Lee, U., Yoo, C. J., Kim, Y. J., and Yoo, Y. M. (2016). Cytotoxicity of gold nanoparticles in human neural precursor cells and rat cerebral cortex. **Journal of Bioscience and Bioengineering**. 121(3): 341-344.
- Magnusson, M. H., Deppert, K., Malm, J.-O., Bovin, J.-O., and Samuelson, L. (1999). Gold Nanoparticles: Production, Reshaping, and Thermal Charging. **Journal of Nanoparticle Research**. 1(2): 243-251.
- Mahan, M. M., and Doiron, A. L. (2018). Gold nanoparticles as X-Ray, CT, and multimodal imaging contrast agents: formulation, targeting, and methodology. **Journal of Nanomaterials**. 2018: 1-15.
- Makarov, V. V., Love, A. J., Sinitsyna, O. V., Makarova, S. S., Yaminsky, I. V., Taliansky, M. E., and Kalinina, N. O. (2014). "Green" nanotechnologies: synthesis of metal nanoparticles using plants. **Acta Naturae**. 6(1): 35-44.
- Mangunwardoyo, W., Deasywaty, and Usia, T. (2012). Antimicrobial and identification of active compound *Curcuma xanthorrhiza* Roxb. **International Journal of Basic and Applied Sciences**. 12 (1): 69-78.
- Mannerstrom, M., Zou, J., Toimela, T., Pyykko, I., and Heinonen, T. (2016). The applicability of conventional cytotoxicity assays to predict safety/toxicity of mesoporous silica nanoparticles, silver and gold nanoparticles and multi-walled carbon nanotubes. **Toxicology In Vitro**. 37: 113-120.

- Mishra, A., Kumari, M., Pandey, S., Chaudhry, V., Gupta, K. C., and Nautiyal, C. S. (2014). Biocatalytic and antimicrobial activities of gold nanoparticles synthesized by *Trichoderma sp.* **Bioresour Technology**. 166: 235-242.
- Mittal, A. K., Chisti, Y., and Banerjee, U. C. (2013). Synthesis of metallic nanoparticles using plant extracts. **Biotechnology Advances**. 31(2): 346-356.
- Mocan, L. (2013). Drug delivery applications of gold nanoparticles. **Biotechnology, Molecular Biology And Nanomedicine**. 1 No.1: 1-6.
- Nadaf, N. Y., and Kanase, S. S. (2016). Biosynthesis of gold nanoparticles by *Bacillus marisflavi* and its potential in catalytic dye degradation. **Arabian Journal of Chemistry**. xxx. xxx-xxx: 1-9.
- Naraginti, S., and Li, Y. (2017). Preliminary investigation of catalytic, antioxidant, anticancer and bactericidal activity of green synthesized silver and gold nanoparticles using *Actinidia deliciosa*. **Journal of Photochemistry and Photobiology B**. 170: 225-234.
- Nguyen, D. T., Kim, D.-J., and Kim, K.-S. (2011). Controlled synthesis and biomolecular probe application of gold nanoparticles. **Micron**. 42(3): 207-227.
- OECD. (2013). *Test No. 236: Fish Embryo Acute Toxicity (FET) Test*: OECD Publishing.
- Okitsu, K., Ashokkumar, M., and Grieser, F. (2005). Sonochemical synthesis of gold nanoparticles: effects of ultrasound frequency. **The Journal of Physical Chemistry B**. 109(44): 20673-20675.
- Paino, I. M., Marangoni, V. S., de Oliveira Rde, C., Antunes, L. M., and Zucolotto, V. (2012). Cyto and genotoxicity of gold nanoparticles in human hepatocellular

- carcinoma and peripheral blood mononuclear cells. **Toxicol Letters**. 215(2): 119-125.
- Pan, Y., Leifert, A., Ruau, D., Neuss, S., Bornemann, J., Schmid, G., Brandau, W., Simon, U., and Jähnen-Dechent, W. (2009). Gold nanoparticles of diameter 1.4 nm trigger necrosis by oxidative stress and mitochondrial damage. **Small**. 5(18): 2067-2076.
- Parsons, J., Peralta-Videa, J., and Gardea-Torresdey, J. (2007). *Chapter 21 Use of plants in biotechnology: Synthesis of metal nanoparticles by inactivated plant tissues, plant extracts, and living plants* (Vol. 5).
- Paul, B., Bhuyan, B., Purkayastha, D. D., and Dhar, S. S. (2016). Photocatalytic and antibacterial activities of gold and silver nanoparticles synthesized using biomass of *Parkia roxburghii* leaf. **Journal of Photochemistry and Photobiology B**. 154: 1-7.
- Pileni, M. P. (1997). Nanosized particles made in colloidal assemblies. **Langmuir**. 13(13): 3266-3276.
- Pimprikar, P. S., Joshi, S. S., Kumar, A. R., Zinjarde, S. S., and Kulkarni, S. K. (2009). Influence of biomass and gold salt concentration on nanoparticle synthesis by the tropical marine yeast *Yarrowia lipolytica* NCIM 3589. **Colloids Surf B Biointerfaces**. 74(1): 309-316.
- Prasad, B. L. V., Stoeva, S. I., Sorensen, C. M., Zaikovski, V., and Klabunde, K. J. (2003). Gold nanoparticles as catalysts for polymerization of alkylsilanes to siloxane nanowires, filaments, and tubes. **Journal of the American Chemical Society**. 125(35): 10488-10489.

- Pulaski, B. A., and Ostrand-Rosenberg, S. (2001). Mouse 4T1 breast tumor model. *Curr Protoc Immunol, Chapter 20, Unit 20.22.*
- Pyati, U. J., Look, A. T., and Hammerschmidt, M. (2007). Zebrafish as a powerful vertebrate model system for in vivo studies of cell death. **Seminars in Cancer Biology.** 17(2): 154-165.
- Rajan, A., Vilas, V., and Philip, D. (2015). Studies on catalytic, antioxidant, antibacterial and anticancer activities of biogenic gold nanoparticles. **Journal of Molecular Liquids.** 212: 331-339.
- Rajeshkumar, S. (2016). Anticancer activity of eco-friendly gold nanoparticles against lung and liver cancer cells. **Journal of Genetic Engineering and Biotechnology.** 14(1): 195-202.
- Ramachandran, R., Krishnaraj, C., Sivakumar, A. S., Prasannakumar, P., Abhay Kumar, V. K., Shim, K. S., Song, C. G., and Yun, S. I. (2017). Anticancer activity of biologically synthesized silver and gold nanoparticles on mouse myoblast cancer cells and their toxicity against embryonic zebrafish. **Materials Science & Engineering. C, Materials for Biological Applications.** 73: 674-683.
- Saha, B., Bhattacharya, J., Mukherjee, A., Ghosh, A., Santra, C., Dasgupta, A. K., and Karmakar, P. (2007). *In vitro* structural and functional evaluation of gold nanoparticles conjugated antibiotics. **Nanoscale Research Letters.** 2(12): 614-622.
- Saha, K., Agasti, S. S., Kim, C., Li, X., and Rotello, V. M. (2012). Gold nanoparticles in chemical and biological sensing. **Chemical Reviews.** 112(5): 2739-2779.

- Salleh, N. A., Ismail, S., and Ab Halim, M. R. (2016). Effects of *Curcuma xanthorrhiza* extracts and their constituents on phase II drug-metabolizing enzymes activity. **Pharmacognosy Research**. 8(4): 309-315.
- Santhosh, S. B., Ragavendran, C., and Natarajan, D. (2015). Spectral and HRTEM analyses of *Annona muricata* leaf extract mediated silver nanoparticles and its larvicidal efficacy against three mosquito vectors *Anopheles stephensi*, *Culex quinquefasciatus*, and *Aedes aegypti*. **Journal of Photochemistry and Photobiology B**. 153: 184-190.
- Sastry, M., Ahmad, A., Islam Khan, M., and Kumar, R. (2003). *Biosynthesis of metal nanoparticles using fungi and actinomycete* (Vol. 85).
- Schaal, P. A., Besmehn, A., Maynicke, E., Noyong, M., Beschoten, B., and Simon, U. (2012). Electrically conducting nanopatterns formed by chemical e-beam lithography via gold nanoparticle seeds. **Langmuir**. 28(5): 2448-2454.
- Shah, M., Badwaik, V., Kherde, Y., Waghwan, H. K., Modi, T., Aguilar, Z. P., Rodgers H., Hamilton, W., Marutharaj, T., Webb, C., Lawrenz, M. B., and Dakshinamurthy, R. (2014). Gold nanoparticles: various methods of synthesis and antibacterial applications. **Frontiers in Bioscience (Landmark Edition)**. 19: 1320-1344.
- Shah, M., Fawcett, D., Sharma, S., Tripathy, K. S., and Poinern, E. G. (2015). Green synthesis of metallic nanoparticles via biological entities. **Materials**. 8(11): 7278-7308.
- Shameli, K., Ahmad, M. B., Zamanian, A., Sangpour, P., Shabanzadeh, P., Abdollahi, Y., and Zargar, M. (2012). Green biosynthesis of silver nanoparticles using

Curcuma longa tuber powder. **International Journal of Nanomedicine**. 7: 5603-5610.

Sharma, S., Bora, P. J., Gogoi, P., Boruah, R., Mohan, K. K., and Dolui, S. (2015). *Plasmonic bulk heterojunction photovoltaic devices based on poly (9-vinylcarbazole)/gold nanocomposites: effect of aspect ratio of gold nanorod* (Vol. 26).

Shukla, R., Bansal, V., Chaudhary, M., Basu, A., Bhonde, R. R., and Sastry, M. (2005). Biocompatibility of gold nanoparticles and their endocytotic fate inside the cellular compartment: a microscopic overview. **Langmuir**. 21(23): 10644-10654.

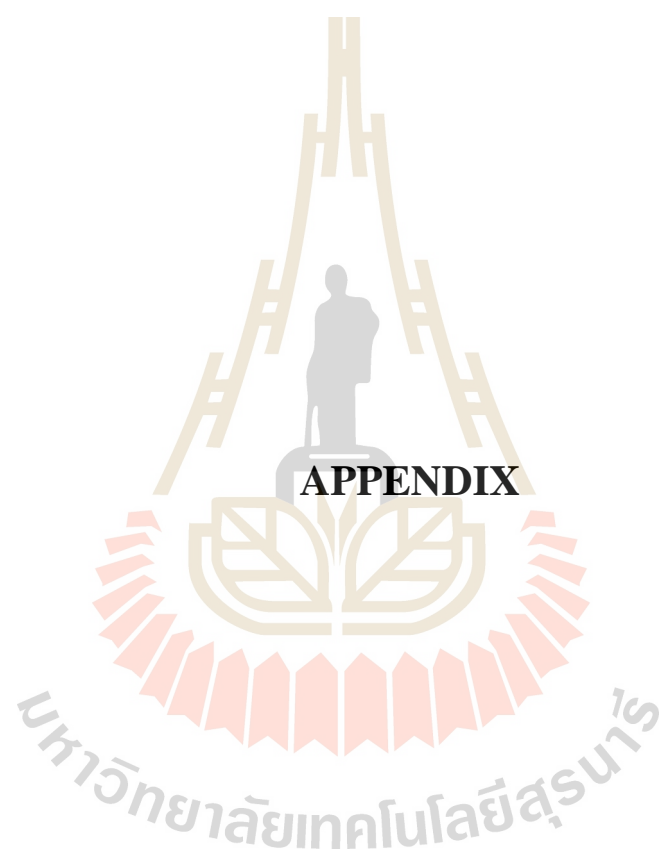
Singh, A. K., Talat, M., Singh, D. P., and Srivastava, O. N. (2010). Biosynthesis of gold and silver nanoparticles by natural precursor clove and their functionalization with amine group. **Journal of Nanoparticle Research**. 12(5): 1667-1675.

Sujitha, M. V., and Kannan, S. (2013). Green synthesis of gold nanoparticles using Citrus fruits (*Citrus limon*, *Citrus reticulata* and *Citrus sinensis*) aqueous extract and its characterization. **Spectrochimica Acta A: Molecular and Biomolecular Spectroscopy**. 102: 15-23.

Sun, S., Mendes, P., Critchley, K., Diegoli, S., Hanwell, M., Evans, S. D., Leggett, G.J., Preece, J.A., and Richardson, T. H. (2006). Fabrication of gold micro- and nanostructures by photolithographic exposure of thiol-stabilized gold nanoparticles. **Nano Letters**. 6(3): 345-350.

Thompson, D. T. (2007). Using gold nanoparticles for catalysis. **Nano Today**. 2(4): 40-43.

- Truong, L., Saili, K. S., Miller, J. M., Hutchison, J. E., and Tanguay, R. L. (2012). Persistent adult zebrafish behavioral deficits results from acute embryonic exposure to gold nanoparticles. **Comparative Biochemistry and Physiology-Part C: Toxicology & Pharmacology**. 155(2): 269-274.
- Villiers, C., Freitas, H., Couderc, R., Villiers, M. B., and Marche, P. (2010). Analysis of the toxicity of gold nano particles on the immune system: effect on dendritic cell functions. **Journal of Nanoparticle Research**. 12(1): 55-60.
- Yiing Yee, F., Periasamy, V., and Abd Malek, S. N. (2014). *Green synthesis of gold nanoparticles using aqueous ethanol extract of Curcuma mangga rhizomes as reducing agent* (Vol. 1657).
- Zhao, P., Li, N., and Astruc, D. (2013). State of the art in gold nanoparticle synthesis. **Coordination Chemistry Reviews**. 257(3): 638-665.
- Zhou, Y., Lin, W., Huang, J., Wang, W., Gao, Y., Lin, L., Li, Q., Lin, L., and Du, M. (2010). Biosynthesis of gold nanoparticles by foliar broths: roles of biocompounds and other attributes of the extracts. **Nanoscale Research Letters**. 5(8): 1351-1359.



APPENDIX

PREPARATION OF REAGENTS

1. DMEM medium

DMEM (1X) with high glucose, L-glutamine, phenol red	1	pack
NaHCO ₃	2.0	g
Distilled water	800	ml
Adjust pH 7.4 and then adjust volume to 1,000 ml		
Add 100 U/ml antibiotic-antimycotic	10.0	ml

2. MTT solution (0.5 mg/ml)

MTT powder	2.50	mg
Distilled water	5.0	ml

3. NaBH₄ (0.2 M) solution

NaBH ₄	38.83	mg
Distilled water	5.0	ml

4. PBS (1X)

NaCl	8.00	g
KCl	0.20	g
Na ₂ HPO ₄	1.44	g
KH ₂ PO ₄	0.24	g
Distilled water	800	ml

5. RPMI 1640 medium

RPMI 1640 (1X) with L-glutamine, phenol red	1	pack
NaHCO ₃	2.00	g
Distilled water	800	ml
Adjust pH 7.4 and then adjust volume to 1,000 ml		
Add 100 U/ml antibiotic-antimycotic	10.0	ml

6. 0.25% trypsin-EDTA solution

2.5% trypsin	5.0	ml
EDTA (10X)	5.0	ml
PBS (1X)	40	ml

7. 0.5 McFarland standard

1% barium chloride	0.05	ml
1% sulfuric acid	9.95	ml

CURRICULUM VITAE

Name Mrs. Khairiza Lubis

Date of Birth May 24, 1981

Place of Birth Medan, Indonesia

Education

- State University of Medan, Academic year, 1999-2004: Bachelor of Science (Biology).
- National University of Malaysia, Academic year, 2004-2007: Master of Science (Zoology).
- Suranaree University of Technology, Academic year, 2014-2018: Upon acceptance of this thesis, she will graduate with a Doctor of Philosophy in Environmental Biology from Suranaree University of Technology.

Grants SUT-Ph.D. Scholarship Program for ASEAN, 2014-2017.